January 2014

Agricultural Drought Monitoring And Prediction Using Soil Moisture Deficit Index

Jiexia Wu

AGRICULTURAL DROUGHT MONITORING AND PREDICTION USING SOIL
MOISTURE DEFICIT INDEX

by

Jiexia Wu
Bachelor of Science, Zhejiang University of Technology, 2008
Master of Science, University of Twente, 2010

A Thesis

Submitted to the Graduate Faculty
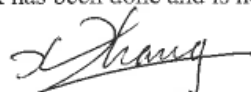

of the

University of North Dakota

In partial fulfillment of the requirements

for the degree of

Master of Science

Grand Forks, North Dakota
May 2014

This thesis, submitted by Jiexia Wu in partial fulfillment of the requirements for the Degree of Master of Science from the University of North Dakota, has been read by the Faculty Advisory Committee under whom the work has been done and is hereby approved.
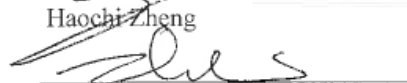
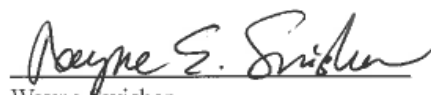_____
Xiaodong zhang

_____
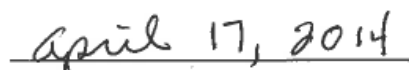Andrie Kirilenko

_____
Haochi Zheng

_____
Zhulu Lin

This thesis meets the standards for appearance, conforms to the style and format requirements of the Graduate School of the University of North Dakota, and is hereby approved.

_____
Wayne Swisher
Dean of the Graduate School

_____
April 17, 2014
Date

ii

PERMISSION

Title   Agricultural drought monitoring and prediction using soil moisture
                 deficit index

Department   Earth System Science and Policy

Degree   Master of Science

In presenting this thesis in partial fulfillment of the requirements for a graduate degree from the University of North Dakota, I agree that the library of this University shall make it freely available for inspection. I further agree that permission for extensive copying for scholarly purposes may be granted by the professor who supervised my thesis work or, in his absence, by the chairperson of the department or the dean of the Graduate School. It is understood that any copying or publication or other use of this thesis or part thereof for financial gain shall not be allowed without my written permission. It is also understood that due recognition shall be given to me and to the University of North Dakota in any scholarly use which may be made of any material in my thesis.

                                              Jiexia Wu

                                              Date: March 24, 2014

TABLE OF CONTENTS

LIST OF FIGURES

LIST OF TABLES

ACKNOWLEDGEMENTS

My deepest gratitude goes first and foremost to my first supervisor Dr. Xiaodong Zhang, for his constant encouragement and professional instructions. During the preparation of the thesis, he provided me with inspiring advice and corrected my writing mistakes carefully. Without his pushing me ahead, the completion of this thesis would be impossible.

Grateful acknowledgement is made to my committee members Dr. Haochi Zheng, Dr. Andrei Kirilenko and Dr. Zhulu Lin whose suggestions I always benefited a lot. They are warm-hearted and always ready for help. During my thesis work, they gave gave very insight suggestions on modeling and data analysis.

I would like to express my gratitude to all the friends I met in ESSP. It is an unforgettable experience to study and live with a group of professional people with diverse backgrounds. I deeply appreciate the contribution to this thesis made in various ways by professors in ESSP Department who gave the basic knowledge of remote sensing, GIS, ecosystem, sustainable energy, environmental policy and economics, hydrology, climate change and geology. I also appreciate the help from my friends and colleagues Qiang Zhou, Michael Knudson, Sergey Molodstov, Tatiana Molodstova, Rob Proulx, Gehendra Kharel and Eric Castle who I spent most of my life with in ESSP. Thank you for making my life colorful.

ABSTRACT

The purposes of this study are: 1) to evaluate the performance of an agricultural drought index, Soil Moisture Deficit Index (SMDI) at continental scale; 2) to develop an agricultural drought prediction method based on precipitation, evapotranspiration and terrestrial water storage.

This study applied multiple linear regression (MLR) with the inputs of precipitation from Parameter-elevation Regressions on Independent Slopes Model (PRISM), evapotranspiration from Moderate Resolution Imaging Spectroradiometer (MODIS) MOD 16 and terrestrial water storage (TWS) derived from the Gravity Recovery and Climate Experiment (GRACE) to predict soil moisture and SMDI. The inputs of the MLR model were chosen based on the mass conservation of the hydrological quantities at the near surface soil layer (two meters). In addition, the model also includes seasonal and regional terms for estimation.

Comparisons with the US drought monitor （USDM）showed that SMDI can be used as a proxy of agricultural drought. The model exhibited strong predictive skills at both one- and two-month lead times in forecasting agricultural drought (correlation >0.8 and normalized root mean square error <15%).

CHAPTER I

INTRODUCTION

Droughts usually occur after a long-term period with low precipitation or high temperature, which causes high evapotranspiration. Lasting conditions of soil moisture deficits can have severe impacts on agricultural production, economics and society (*Clark et al.*, 2002; *Marsh*, 2007). Both observations and models have indicated an increasing number of drought events that probably connect with the global climate change (*Dai*, 2011). In the United States, the loss due to drought is about $6-$8 billion per year (*Federal Emergency Management Agency*, 1995). However, the recent drought that afflicted nearly the entire North America continent and lasted almost two years from 2010 to 2012 (*Freedman*, 2012) had affected the agricultural production severely. For example, just the 2011 agricultural loss in Texas alone already exceeded 7 billion (*Walsh*, 2011). One of the possible reasons for the high cost is lack of recognition of drought events, because drought develops more slowly than other disasters such as floods and hurricanes and it is hard to recognize drought until it becomes severe (*Luo and Wood*, 2007).

Drought can be categorized into four categories: meteorological drought, agricultural drought hydrological drought and socio-economic drought (*Mishra and Singh*, 2010; *Wilhite and Glantz*, 1985). Meteorological drought results from a lack of

precipitation over a long time period. Therefore precipitation deficit is often used as a measure of meteorological drought. Agricultural drought refers to decline of plant water supply and soil moisture deficit. It is the result of precipitation shortage, high actual evapotranspiration, and low level of surface water and groundwater. The most commonly used agricultural drought indicators are the soil moisture deficit (*Mishra and Singh*, 2010). Hydrological drought relates to water shortage in reservoir, stream flow and groundwater. Stream flow data are widely used for hydrological drought evaluation (*Clausen and Pearson*, 1995). Socio-economic drought occurs when water supply fails to meet water demand.

Agriculture sector usually is the first to bear the effect and suffer the most losses (*Palmer*, 1965). The drought events in the 1930s, 1950s, 1980s, and 1990s reveal the vulnerability of agriculture to severe drought (*Pacific Disaster Center*, 2013). Accurately monitoring agricultural drought progression and understanding agricultural drought occurrence, development and recovery can inform drought mitigation plans (*Ntale and Gan*, 2003; *Quiring and Papakryiakou*, 2003) and limit adverse effects (*Sirdas and Sen*, 2003)

Drought indices are used to evaluate drought severity and to inform decision-making. Many drought indices have been developed for agricultural drought evaluation. Soil moisture deficit is a key indicator of agricultural droughts. Sheffield et al (2004) used the current soil moisture percentiles as a measure of an agricultural drought. Another commonly used index is the Crop Moisture Index (*Palmer*, 1968). CMI is constructed based on precipitation excess and soil moisture infiltration, and is suitable for short-term drought monitoring (*Keyantash and Dracup*, 2002). Soil Moisture Deficit

Index (SMDI) (*Narasimhan and Srinivasan*, 2005) was developed based on top layer soil water content to monitor drought evolution based on soil moisture simulated from Soil and Water Assessment Tool (SWAT) model. The results show that the SMDI derived from top 6 feet soil correlates strongly with Palmer Drought Severity Index (PDSI) and Standardized Precipitation Index (SPI-6 months), which indicates that the SMDI in top 6 feet soil layer is able to monitor long term drought. In particular, the SMDI in growing season shows high correlation coefficient (>0.8) with crop yield, and it indicates that the SMDI can be used for agricultural drought monitoring.

Predicting agricultural drought, particularly over large scale, is more difficult than monitoring because of the complex hydrological processes behind it. Few studies have been conducted on agricultural drought prediction at continental or global scale. As for the CONUS, Luo and Wood (2007) (LW07) monitored and predicted agricultural drought based on soil moisture percentile derived from a model-based Drought Monitoring and Prediction System (DMAPS) using a land surface model, Variable Infiltration Capacity (VIC). The DMAPS predictions generally compared well with real time drought monitoring from the USDM. However, in the most recent drought event, their products showed an obvious disagreement with the observation from USDM in spring 2012. Figure 1 shows an example of comparing the LW07 drought prediction with and USDM for March 2012. While there is an overall agreement between the two, a noticeable discrepancy was observed in New Mexico and Texas. Similar difference in this region is also observed in other months of early 2012.
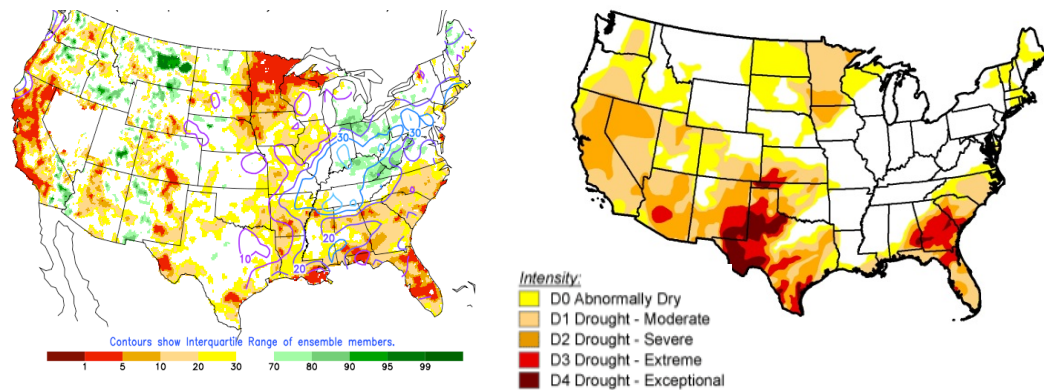
Figure 1 Drought prediction by LW07 and drought monitoring from US Drought Monitor over the CONUS in March 2012

In this study, we developed an agricultural drought prediction method and validated the model using the recent drought event from 2010 to 2012. We used SMDI as a proxy for agricultural drought. Drought prediction was based on an MLR model with observed data as explanatory variables.

Research Objectives

The research objectives are to evaluate the performance of SMDI in the 2010 to 2012 drought over the CONUS and to develop a prediction method to improve the understanding of drought events.

Drought monitoring

- Examine the performance of SMDI by comparing it with US drought monitor products

- Evaluate spatial and temporal evolution of 2010 to 2012 drought in top layer soil (SMDI)

Drought prediction

- Using MLR to estimate soil moisture change based on meteorological and hydrological variables

- Develop drought prediction using the current SMDI values and predicted soil moisture change.

Thesis Outlines

Chapter 2 provides a review of existing literature on drought definition, classifications. Since soil moisture is the key indicator of agricultural drought, it also outlines the three major ways of soil moisture retrieval. In addition, drought prediction methods are also presented.

Chapter 3 describes the study area and data. It introduces the general climate conditions of the CONUS, including precipitation and temperature. Land cover and soil moisture were also briefly introduced in this chapter. Data used in this study are also listed in this chapter.

Chapter 4 is the methodology of drought monitoring and prediction. In this section, the method of SMDI calculation and MLR model are introduced.

Chapter 5 shows the results and discussion of drought monitoring and prediction using SMDI and the comparison between SMDI and US drought monitor.

Chapter 6 is conclusions and recommendations.

CHAPTER II

LITERATURE REVIEW

Definitions of drought

Drought usually happens after a period of aberrant dry weather and it gradually impacts vegetation growth, water supply and economics. The occurrences of droughts are related not only to metrological processes but also to hydrological processes or even human activities. Since drought is not just a physical phenomenon, it can be defined both conceptually and operationally (*Wilhite and Glantz*, 1985). Conceptually, drought is a general term, which gives people knowledge of the disaster. At the same time, conceptual drought also helps in decision-making. Operational definition helps to understand the evolution of drought, for example, the occurrence, development and recovery of drought. The operational definition also includes the drought characteristics such as duration, severity, magnitude, intensity, geographic extent and frequencies for a given time period.

For those drought characteristics analysis the meteorological components such as hourly, daily and monthly precipitation, surface temperature and the hydrological variables such as evapotranspiration, wind speed are needed. Drought monitoring is difficult, because the impact of drought differs from region to region, and no single drought index applies in all circumstances.

Generally, drought can be categorized into four classes based on the impacts: meteorological, agricultural, hydrological and socio-economic drought (*Mishra and Singh*, 2010; *Wilhite and Glantz*, 1985). Among the four drought classes, there is a particular order for occurrence, as shown in Figure 2. Precipitation shortage is usually the measure of meteorological drought and precipitation deficit for a long period causes soil moisture content decrease (agricultural drought). Low recharge from soil decreases the water amount in stream flow and reservoirs (hydrological drought).
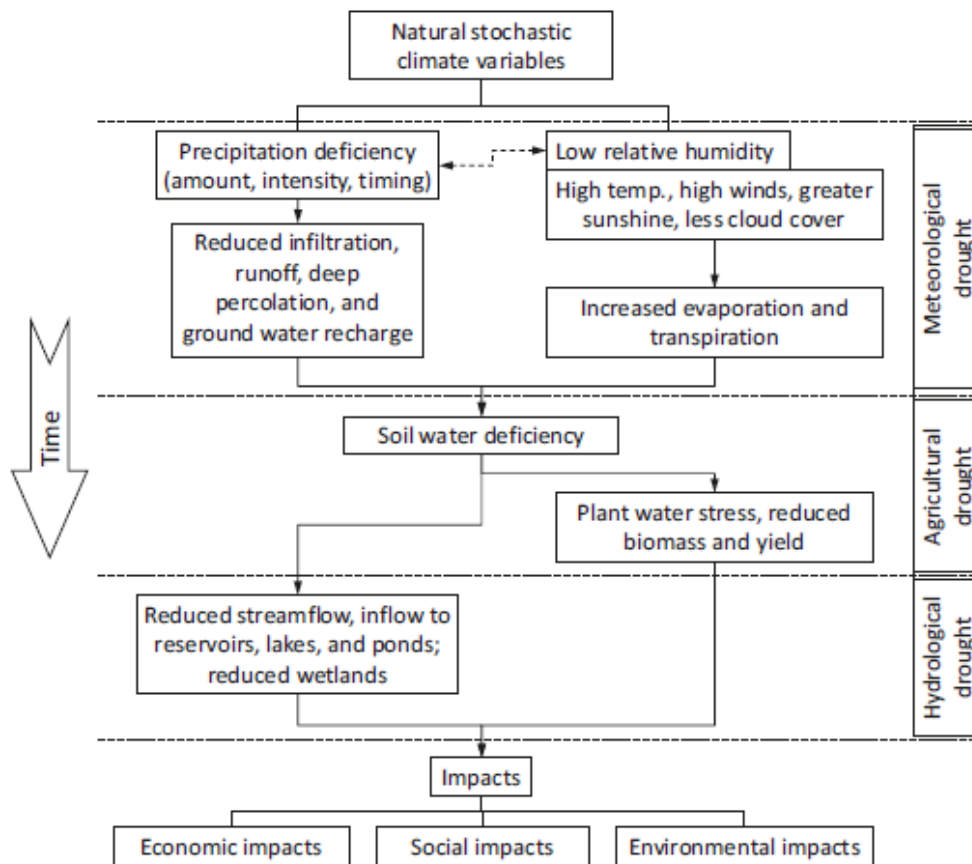
Figure 2 The general sequence of drought occurrence (*NDMC*, 2006)

Meteorological drought

Meteorological drought occurs when an area experiences a lack of precipitation over an extended period of time. Several studies on meteorological drought were based on monthly precipitation data or cumulative precipitation shortages (*Chang and Kleopa*, 1991; *Santos*, 1983). For example, rainfall deciles estimate the rank of current monthly precipitation in historical rainfall records (*Gibbs and Maher*, 1967) to identify wetness conditions; the standardized precipitation index (SPI) calculates the probability of precipitation for time periods ranging from one month (short-term) to twenty-four months (long-term) (*McKee et al.*, 1993a); the Cumulative Precipitation Anomaly (*Hayes et al.*, 1999) compares rainfall shortage with long-term mean values to identify the current drought severity; the Rainfall Anomaly Index (RAI) (*Van Rooy*, 1965) gives the information of regional drought based on historical precipitation distribution. Among the many indices used to evaluate drought, the most commonly used drought index is Palmer Drought Severity Index (PDSI) (*Palmer*, 1965). The PDSI is used by the United States Department of Agriculture (USDA) and state government to assess and communicate drought conditions on a broad scale. The idea of Palmer's work was based on water balance among precipitation, evapotranspiration, soil recharge, runoff, and soil moisture with other auxiliary data such as temperature.

Agricultural drought

Soil moisture is the key indicator as such agricultural drought indices are often based on soil moisture deficit analysis. Many researchers use soil moisture as a proxy to study drought evolution. Soil Moisture Deficit Index (SMDI) was developed to quantify drought severity (*Narasimhan and Srinivasan*, 2005). They used weekly soil moisture

data derived from Soil and Water Assessment Tool (SWAT) hydrological model to calculate SMDI, which was found correlated well with SPI and PDSI. The calculated SMDI also showed high correlation (r >0.75) with the wheat and sorghum crop yields within the study area.. Later, the SMDI method was also applied to GRACE TWS (*Agboma et al.*, 2009; *Yirdaw et al.*, 2008) to estimate Total Storage Deficit Index (TSDI). Their study illustrated that the TSDI was able to characterize the 2002/2003 drought in the Canadian Prairie, and they also suggested that TSDI had the ability to monitor drought in regions sharing the similar hydrological and geological complexities. Another commonly used agricultural drought index is the Crop Moisture Index (*Palmer*, 1968). The CMI uses precipitation excess and soil moisture infiltration to monitor drought situations and is very suitable to short-term droughts (*Keyantash and Dracup*, 2002). Rhee et al (2010) developed Scaled Drought Condition Index (SDCI) with land surface temperature, Normalized Difference Vegetation Index, and precipitation for agricultural drought monitoring. The spatial and temporal distribution of SDCI agreed to the USDM maps in both arid regions (Arizona and New Mexico) and humid regions (North Carolina and South Carolina). Although first designed as a meteorological drought index, PDSI is more suited for agricultural and hydrological drought monitoring, because it changes slowly and is not so sensitive to the change of short term weather conditions for example a heavy rainfall event (*Alley*, 1984).

Hydrological drought

Hydrological drought is more related to surface and subsurface water storage. The most common indices are Hydrological Drought Severity Index (PHDI) and the Surface Water Supply Index (SWSI). PHDI was first introduced by Palmer (1968). The basic idea

of PHDI is similar to PDSI, but it depends more on previous climate conditions because hydrological drought often have longer memories than meteorological drought. SWSI combined climatologic and hydrological characteristics and was developed to include snow accumulation and to estimate drought in large mountainous areas. The SWSI is a good indication on catchment scale while having a disadvantage when used for inter-basin comparison (*Hayes et al.*, 1999).

Socio-economic drought

Socio-economic drought is defined as water supply, which fails to meet the demand (*Mishra and Singh*, 2010). It is often used for water resources planning and management.

Comparison of the commonly used drought indices

The most commonly used drought indices are PDSI, SPI, SWSI and CMI.

PDSI is derived by water balance algorithm and the calculation of PDSI is based on precipitation, daily air temperature, available water content. PDSI changes slowly because it highly relies on antecedent conditions. The equation used to calculate PDSI is:

$$X_i = \frac{Z_i}{3} + 0.897 X_{i-1} \quad (1)$$

Where X is PDSI, Z value is the current soil moisture condition. From the equation, about 90% of the current PDSI estimate is carried over from the previous month. Meteorological drought always lasts for a short period while agricultural and hydrological drought show longer memory, therefore although the PDSI was denoted to estimate meteorological drought, it was more appropriate to measure agricultural and hydrological drought (*Alley*, 1984).

PDSI has some limitations. Palmer (1965) divided the soil into two layers, and he assumed that water transferred from the top soil layer to second layer only when the top

layer is fully saturated. Runoff only occurs when the two soil layers are saturated (*Quiring and Papakryiakou*, 2003). However, in reality, more factors affect runoff such as soil type and land use, causing inaccurate estimation of runoff. Another limitation of PDSI is that it considers all precipitation as rainfall, which may lead to significant errors in northern areas with snow cover in winter.

The SPI (*McKee et al.*, 1993b) measures meteorological drought. It uses standardized observation of precipitation at different durations from 3 to 48 months to evaluate shortterm and longterm drought. The duration of months is used for agricultural purpose and also as a reference for water supply and management (*Guttman*, 1999; *Quiring and Papakryiakou*, 2003). SPI only uses precipitation data and it does not account for other factors such as soil, land cover and temperature. For agricultural drought purposes, soil moisture in root zone is more suited. Therefore, SPI is not a good measure of agricultural drought.

SWSI was first developed for Colorado to complement PDSI by including the information of surface water such as reservoir storage and stream flow (*Wilhite and Glantz*, 1985). For irrigated land, SWSI is a good indicator for agricultural drought monitoring. However, irrigated land only account for 7.5% of the US according to Economic Research Service (2013) at USDA in 2007. Most of the croplands and pasturelands rely on local precipitation, therefore the use of SWSI is not good for agricultural drought.

CMI was first developed by Palmer (*Palmer*, 1968) with PDSI. PDSI was developed for long-term monitoring and CMI was designed to estimate short-term moisture conditions in major crop-producing regions. CMI was calculated by combining

CMI in previous week and current precipitation and air temperature. Compared with PDSI, CMI is more sensitive to short term weather change, for example CMI may change rapidly with a heavy rainfall event. Therefore, CMI is not a good indicator for long term drought monitoring. Both PDSI and CMI do not consider land use and land cover in water balance algorithm.

A good drought index should be appropriate in both short term (several months) and long term (several years) drought monitoring. The inputs of the indices should well describe the moisture conditions in root zone (*Narasimhan and Srinivasan*, 2005). The SMDI (*Narasimhan and Srinivasan*, 2005) was developed from a comprehensive hydrological model, SWAT, which uses spatially distributed data of soil, land use, digital elevation model and climate data for modeling. The SMDI shows its ability in both short-term and long-term drought monitoring by comparable results with PDSI and SPI.

The SMDI in growing season also shows high correlation coefficient with crop yield. Therefore SMDI is appropriate for agricultural drought.

Soil moisture estimation

Accurate estimate of soil moisture is important for monitoring and predicting agricultural drought. Soil moisture content is mainly measured from in situ instruments, model simulation, and remote sensing observations.

In situ measurements

The most accurate method is based on sampling that can be considered as point data.

The methods to measure soil moisture include gravimetric, radioactive and capacitive techniques (*Walker et al.*, 2004). The gravimetric method is taking the volume of the soil sample, weight it before and after drying in an oven, and calculate the percentage of soil moisture loss from the sample. The gravimetric method is accurate but time consuming; therefore, it is usually used for soil moisture calibration. Radioactive method is based on radioactive transmissions. The most commonly used probe is Neutron Probe, which can be installed in the field permanently. But due to the differences of soil properties, soil moisture readings from Neutron Probe needs calibration. The instruments such as Time Domain Reflectrometry (TDR) provide soil moisture percentage by measuring the dielectric properties of the soil (*Baker and Allmaras*, 1990; *Ledieu et al.*, 1986). However, since the dielectric properties are also affected by soil organics, porosity and soil types, a calibration is needed for this method (*Roth et al.*, 1992). The drought monitoring purposes, soil moisture content at regional or global scale is required. However, because of soil moisture spatial variability results from many variables, such as land cover, topography, soil texture (*Bosch et al.*, 2006); point scaled soil moisture data is not representative to the areal values. Therefore, it is impossible to use in situ point soil moisture data to evaluate agricultural drought on large scale.

Model simulations

Land surface models can provide areal soil moisture information at different soil layers. For agricultural drought monitoring, soil moisture at root zone is important. Since plants root depths range from several centimeters to several meters, the soil moisture data at top soil layer (<10cm) from in-situ measurements or most of the remote sensing products are not sufficient. Therefore model based soil moisture is more suited for

agricultural drought.

The Global Land Data Assimilation System (GLDAS) is a land surface modeling system (LSM) integrates satellite and ground based observations to simulate a variety of geophysical variables (*Rodell et al.*, 2004a). At the time of this study, GLDAS incorporated four LSM's: Mosaic (*Koster and Suarez*, 1992), Common Land Model (*Dai et al.*, 2003), National Centers for Environmental Prediction/Oregon State University/Air Force/Hydrologic Research Lab Model (NOAH; *Chen et al.*, 1996), and Variable Infiltration Capacity (VIC; *Liang et al.*, 1994b). LSM simulates water and heat interactions between biosphere, atmosphere and hydrosphere. The first LSM model was developed in the 1970s (*Manabe*, 1969). It was a bucket model and considered only the most basic water balance process, such as rainfall, runoff, and evaporation. In the 1980s the models become more complicated and combined more climate and hydrological components. These models also consider multiple soil layers (*McCumber and Pielke*, 1981). Later in the 1990s, the development of Mosaic (*Koster and Suarez*, 1992) and VIC (*Liang et al.*, 1994a) allowed global simulation .

The NOAH LSM was an amalgam of diurnally dependent Penman potential evaporation, a four-layer soil model (*Mahrt and Pan*, 1984) and the primitive canopy model (*Pan and Mahrt*, 1987). During the past twenty years, the model has been constantly improved, including the surface runoff process (*Schaake et al.*, 1996), frozen soil moisture, and snow pack which make it applicable in cold regions during winter (*Ek et al.*, 2003), and the bare soil evaporation (*Noilhan and Planton*, 1989). These improvements significantly enhanced the performance of the NOAH LSM, which has been validated in many regions with different climatic, hydrological and geological

conditions. Sridhar et al (2002) validated NOAH LSM by using Oklahoma Atmospheric Surface-Layer Instrumentation System (OASIS) measurements of net radiation, latent heat flux sensible heat flux and ground heat flux and found relatively low root mean square errors (RMSEs) in Oklahoma region. Chen et al (2003) evaluated NOAH model by using both surface and aircraft measurements and found that the model is able to capture the land surface heterogeneity which closely relates to land use and soil moisture. Fan et al (2006) compared NOAH LSM simulated soil moisture with observed data in Illinois and found the correlation coefficient higher than 0.7 at all three tested regions and correlation coefficient between the observed and simulated soil moisture in four vertical layer are higher than 0.6.
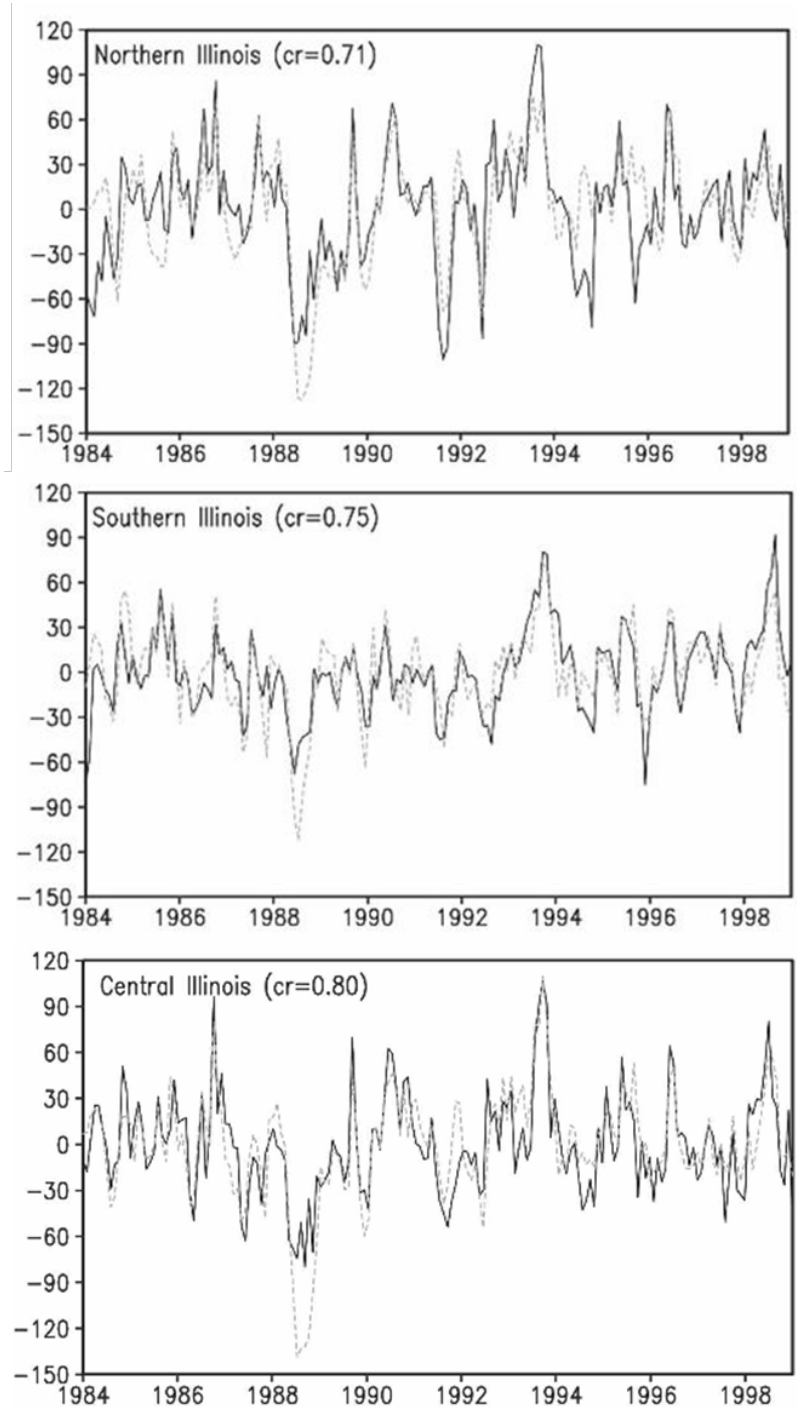
Figure 3 Comparison of soil moisture temporal variability between NOAH LSM simulation and observation in Illinois. Dash lines are observed soil moisture and solid lines are simulated soil moisture. Y-axis is soil moisture anomaly (mm). Correlation coefficients are above 0.7 (Fan et al., 2006).

Remote sensing

The development of remote sensing technology offered the feasibility of soil moisture content measurement by optical, thermal infrared, passive and active microwave remote sensing techniques (*Walker*, 1999). The differences of these techniques are the wavelengths of the electromagnetic spectrum of the energy. All of them have their own advantages and disadvantages depending on whether the surface is sensitive to the electromagnetic radiation. The sensors measure the response and relate it to soil water content. Since sensors cannot directly measure soil moisture, physical, empirical and semi-empirical methods are used to translate the signals received to soil moisture.

Optical remote sensing uses solar domain from 0.4 to 2.5 μm to measure reflectance (*Sadeghi et al.*, 1984). Although optical remote sensing attracts less attention on soil moisture measurements than microwave remote sensing because of the shorter wavelengths and the impacts of soil organic matter, mineral composition and surface roughness, the relation between soil moisture content and reflectance has been recognized since 1925 (*Angstrom*, 1925). Later several researches focused on creating empirical approaches to describe the relation between them. Bowers and Smith (1972) found a linear relation between soil moisture and water absorption band. Dalal and Henry (1986) measured the relationship between the soil moisture and absorbance in the near infrared band. Rijal et al (2013) developed a model based on Landsat near infrared band to estimate soil moisture in bare land and found a high correlation efficient (r=0.94)with soil water content at 15 cm depth.

Microwave remote sensing estimates soil moisture with the wavelength between 0.5 and 100 cm. Microwave remote sensing for soil moisture measurement is based on

the contrast of dielectric properties of water (>80) and soil particles(<4). Therefore by measuring the emission of the soil the moisture content can be extracted (*Moran et al.*, 2004). There are many microwave sensors for soil moisture monitoring. For example the Advanced Microwave Scanning Radiometer (AMSR-E) flown on Aqua, provides passive microwave measurement. VUA-NASA developed Land Surface Parameter Model (LPRM) using 6.9 GHz and 10.7 GHz channel to retrieve soil moisture from brightness temperature. The Advanced Scatterometers (ASCAT) flown on the MetOP satellite was launched in 2006, and it is an active microwave measurement. ASCAT are successors of ERS to obtain wind speed and direction over ocean globally. Soil moisture information is derived from a change detection method, by Vienna University of Technology (*Figa-Saldaña et al.*, 2002). Backscattering can be simplified to account for soil moisture and vegetation. Here the relative soil moisture is presented from 0%-100% after normalizing to the backscattering coefficient to an incident angle of 40° as being representative for the driest and wettest conditions, respectively. Other sensors working for soil moisture measurement include Special Sensor Microwave/Imager (SMMR), the Tropical Rainfall Measuring Mission Microwave Imager (TRMM-TMI), and the Soil Moisture and Ocean Salinity (SMOS).

Both microwave and optical remote sensing can only measure the soil moisture content in top 5 centimeters at most. GRACE is the only one remote sensing technique that can measure terrestrial water storage from land surface to deep aquifers. GRACE is a satellite mission, launched March 2002, to measure Earth gravity field at various resolutions from 400km to 40,000km every thirty days (*Tapley et al.*, 2004b) over the entire earth surface (*Swenson et al.*, 2003). The GRACE mission has two satellites and

the distance between the two is 220 km with a K-Band microwave system. Both of the two satellites have a Global Positional System (GPS) receiver, which can detect the range change of the satellites and give the information of the positions of the satellites. Unlike other remote sensing products that measure the reflectance or emission from the earth, GRACE measures the rate of change of the distance between two satellites, and the orbit change is partially caused by mass distribution change on earth. These measurements, in turn, are used as a proxy to observe a variety of physical phenomenon, which can be extracted, including values of surface and deep ocean currents, surface water runoff and groundwater storage, and exchanges between ice masses and the ocean (*Wahr et al.*, 1998). GRACE products has been used to obtain different hydrological components, such as groundwater (*Rodell et al.*, 2007; *Rodell and Famiglietti*, 2002; *Tiwari et al.*, 2009), evapotranspiration (*Ramillien et al.*, 2006; *Rodell et al.*, 2004a), and discharge (*Syed et al.*, 2005). GRACE TWS products has been evaluated and compared with different model simulation.

Table 1 Studies comparing simulation results of hydrological models with GRACE TWS data (*Güntner*, 2008)

Study	Focus of study	Hydrological model	GRACE data	GRACE filter	Study area	Temporal variability
(*Andersen et al.*, 2005)	TWS	GLDAS	CSR	Gauss	Central Europe	Inter-annual
(*Andersen and Hinderer*, 2005)	TWS	CPC LaD GLDAS	CSR	Gauss	Global	Inter-annual
(*Hinderer et al.*, 2006)	TWS	LaD GLDAS	CSR	Truncation	Europe	Seasonal
(*Hu et al.*, 2007)	TWS	GLDAS CPC	n.s.	Gauss	Global and Yangtze	Monthly

Table1 cont.

(*Niu et al.*, 2007)	Model	GLDAS-CLM	CSR	Different	Global and selected basins	Monthly
(*Niu and Yang*, 2006)	Model	GLDAS-CLM	CSR	Different	Six largest northern-latitude basins	Monthly
(*Rangelova et al.*, 2007)	TWS	CPC GLDAS LaD	CSR-RL01	Own and Gauss	North America	Monthly
(*Rodell et al.*, 2004b)	ET, TWS	GLDAS	CSR	Gauss	Mississippi	Monthly
(*Schmidt et al.*, 2008)	TWS	WGHM LaD GLDAS	GFZ-RL04	Gauss	Global, Amazon, Mississippi, Ganges	Semi-annual–interannual
(*Syed et al.*, 2008)	TWS	GLDAS-NOAH	CSR-RL01	Gauss	Global and large basins	Monthly, seasonal
(*Tapley et al.*, 2004a)	TWS	GLDAS	CSR	Gauss	Global, South America	Monthly, seasonal
(*Winsemius et al.*, 2006)	TWS	LEW	GFZ-RL03	Gauss	Zambezi	Monthly
(*Famiglietti et al.*, 2011)	GW, TWS	GLDAS	CSR-RL04	Gauss	acramento San Joaquin Basins	Monthly
(*Alkama et al.*, 2010)	model	ISBA-TRIP	CSR-RL04 GFZ-RL04	Gauss	global	Monthly, seasonal
(*Becker et al.*, 2010)	TWS	WGHM	CSR-RL04 GFZ-RL04	Gauss	East Africa	Monthly
(*Li et al.*, 2012)	TWS, model	GLDAS-CLM	CSR-RL04	Gauss	Europe	Monthly
(*Werth and Güntner*, 2010)	model	WGHM	GFZ CSR JPL	Gauss	Global	Monthly
(*Houborg et al.*, 2012)	TWS, model	GLDAS-CLM	CSR-RL04	Gauss	North America	Monthly

Table1 cont.

(*Landerer and Swenson*, 2012)	TWS	GLDAS-NOAH	JPL	Gauss	Global	Monthly
(*Proulx et al.*, 2013)	TWS	GLDAS-NOAH	JPL	Gauss	Northern Glaciated Plain	Monthly

Drought prediction

Drought forecasting is challenging because the occurrence, development and recovery of drought was affected by complex metrological and hydrological processes (*Cordery and McCall*, 2000). The advantage of successfully predicting drought is meaningful to agriculture, especially in agriculture (*Sivakumar and Wilhite*, 2002).

Among all the related processes that cause drought, climatic phenomena such as El Niño Southern Oscillation (ENSO) and the North Atlantic Oscillation (NAO) were often found directly related to drought events in some regions. (*Liu and Juárez*, 2001), and ENSO and NAO have been used as forecasting predictor (*Vogt and Somma*, 2000). The Climate Prediction Center (CPC) releases the information of El Niño and La Niña events and investigated the relation between these phenomena and climate change. They combined several observed global climate phenomena with El Niño/La Niña, the Madden/Julian Oscillation, and atmospheric Tele-connections to improve drought prediction(*Hartmann et al.*, 2002).

For the areas that are not strongly influenced by large-scale climate phenomena, research efforts have been attempted to predict droughts using both statistical- and dynamic-based methods. For example, Luo and Wood (2007) developed a drought monitoring and prediction system over the CONUS through coupling of a regional hydrological model with a global climate model. They used the Variable Infiltration

Capacity land surface model (*Liang et al.*, 1994b), driven by bias corrected and downscaled seasonal forecasts from climate models, to predict soil moisture and agricultural drought. Paulo and Pereira (2007) used Markov chains to predict SPI in several locations in southern Portugal. Karamouz et al (2009) developed a neural network based system to predict drought and its severity using SPI, the Surface Water Supply Index, and PDSI as system inputs.

Most of the drought-prediction-related studies heavily rely upon either model analyses or ground-based measurements (e.g. Paulo and Pereira, (2007); Luo and Wood, (2007)). Satellite observations, which are not yet widely used for drought predictions, have been implemented on a routine basis for estimating terrestrial evapotranspiration (ET) and terrestrial water storage (TWS), both of which are critical hydrological parameters that affect agricultural drought. In particular, on board both the Terra and Aqua satellites, the Moderate Resolution Imaging Spectro-radiometer (MODIS) has a total of 36 spectral channels ranging from the ultraviolet to the infrared spectrum, with a spatial resolution ranging from 250 m to 1 km (*King and Greenstone*, 1999). MODIS ET, which is validated through field measurements (*Mu et al.*, 2011), has been included in one of the standard MODIS land products (MOD16) at both regional and global scales (*Mu et al.*, 2007). Also, being a major source of root zone soil moisture supply, groundwater has been scarcely monitored, and the few measurements that are available are often point-based, leading to a scale "jump" issue in large scale hydrological modeling (*Yeh et al.*, 2006). The Gravity Recovery and Climate Experiment (GRACE), launched in 2002 for measuring subtle changes in Earth's gravity, provide an estimate of changes in terrestrial water storage (TWS) from the land surface to deep aquifers.

GRACE TWS data have been extensively validated (*Rodell et al.*, 2007; *Scanlon et al.*, 2012) and incorporated into land surface models (e.g., *Houborg et al.*, 2012).

MLR is often used to estimate the relation between one or more independent variables and the target variable and is widely used in hydrology. It is based on the best fit in the least squares with minimum sum of squared residuals. Arulsudar et al (2005) predicted daily mean flow data based on MLR with the observation on the Anamur River in the eastern Mediterranean region. Their MLR model results correlate well with the observations (R^2=0.81). Modarres and Sarhadi (2010) predicted the annual extreme hydrological dry spell length of the Halilrud basin in Iran using MLR with the inputs of vegetation cover, maximum elevation of the watershed and the difference between maximum and minimum elevation of watershed. A high correlation coefficient R=0.97 was obtained between the predicted and observed data. As for soil moisture deficit prediction purposes, for example, using an MLR model with meteorological data as explanatory variable was able to predict soil moisture in the top 5 cm of the Danangou catchment in the Loess Plateau of China with an error of 2% (*Qiu et al.*, 2003). High prediction accuracy was obtained when including meteorological data in MLR model for top layer soil moisture forecast.

CHAPTER III

STUDY AREA AND DATA AVAILABILITY

Study area

The study area of this study covers the 48 contiguous states of the U.S. (CONUS) with a total area of 8,080,464.3 km^2.

The United States includes many climate types. In eastern US, the climate types change from humid continental to humid subtropical from north to south. The Great Plains is semi-arid. The climate of the Great Basin, Southwest, California and coastal areas of Oregon and Washington are arid, desert, Mediterranean and oceanic, respectively.

Precipitation

The rainfall amount over the CONUS is quite heterogeneous. In summer and fall, extratropical cyclones result in majority of precipitation in the western and southern US (*Baxter et al.*, 2005). At the same time, the North American monsoon brings the air-mass thunderstorms to southern and eastern of the country (*Adams and Comrie*, 1997). Generally, the average annual precipitation in the eastern US is above 40 inches, which is wetter than the western part. The driest areas are the desert in southwest, northeastern Arizona, Utah and central Wyoming with precipitation amount lower than 20 inches (Figure 4). Figure 5 shows temporal change of monthly averaged precipitation over the CONUS from 2000 to 2012. There is a clear seasonal pattern with high precipitation amount in summer and low values in winter. During this study period from 2003 to 2012,

24

lowest precipitation amount were observed in 2006 and 2012, and the lower than normal

rainfall amount brought drought in these years (Figure 5).

Precipitation: Annual Climatology (1981-2010)
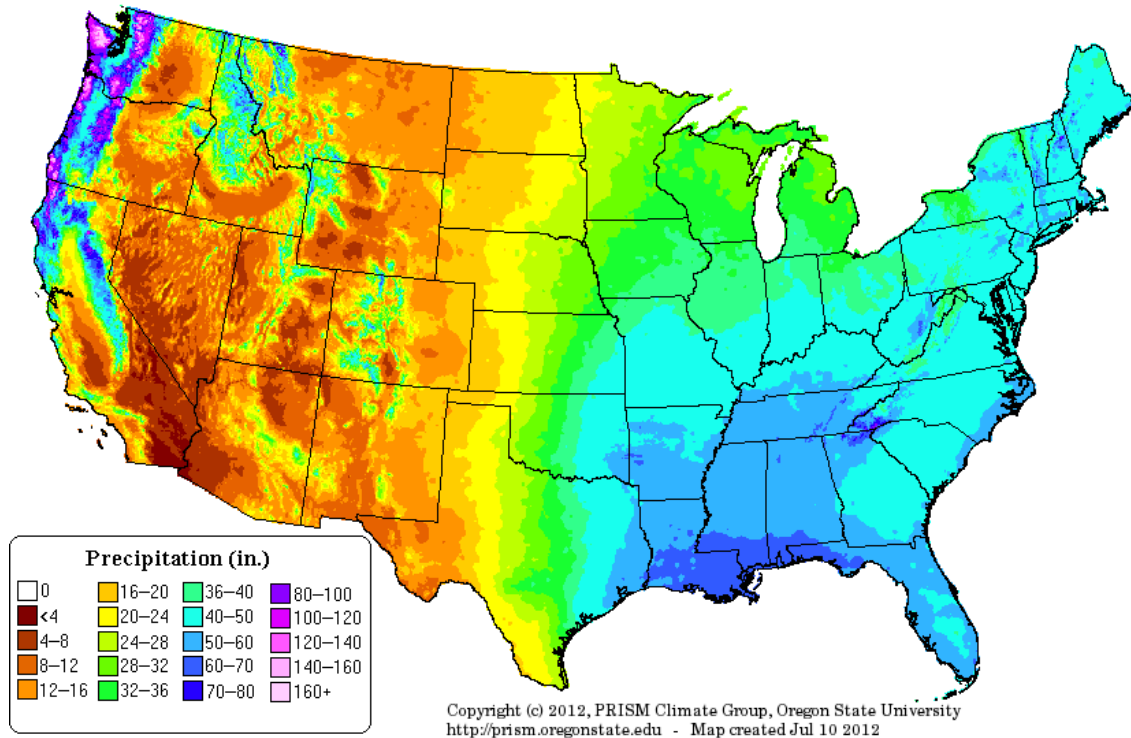
Figure 4 Average annual precipitation from 1981 through 2010. Each color on the maps

represents a range of precipitation values in inches, from just a few to nearly 160 inches.

(Data compiled from PRISM Climate Group source: http://www.prism.oregonstate.edu/)
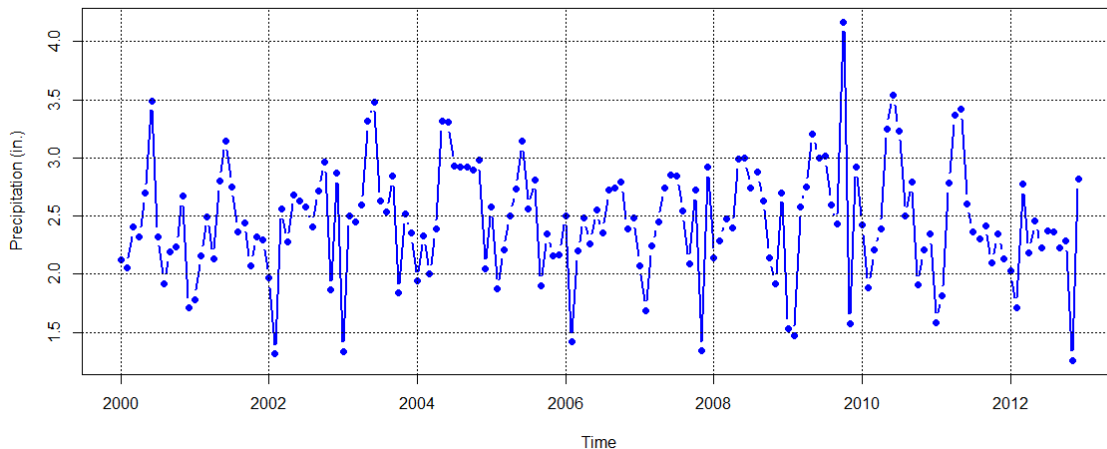
Figure 5 Spatial averaged monthly rainfall rate over the CONUS from 2003 to 2013 (Data source: PRISM Climate Group http://www.prism.oregonstate.edu/)

Temperature

Figure 6 shows the mean air temperature from 1981 to 2010 over the CONUS. Relatively high temperature is recorded in the southern areas. The highest mean temperature was in southern Arizona, Texas and Florida. The average air temperature in these areas is above 70°F. The average air temperature in the northeastern areas is relatively lower about 35°F. The historical extreme high temperature was recorded in Nevada about 125°F on June 29, 1994 and the lowest temperature was recorded in Montana about -70°F on January 20, 1954 (*NCDC*, 2006). Air temperature is quite important in hydrological processing. Together with solar radiation, air humidity and wind speed, air temperature is a crucial climatological parameter to evaluate evapotranspiration on land. Spatial averaged near surface temperature shows clear seasonal pattern, with high temperature about 75K in summer and 30K in winter (Figure 7).

30-yr Normal Mean Temperature: Annual
Period: 1981-2010

Copyright (c) 2013, PRISM Climate Group, Oregon State University
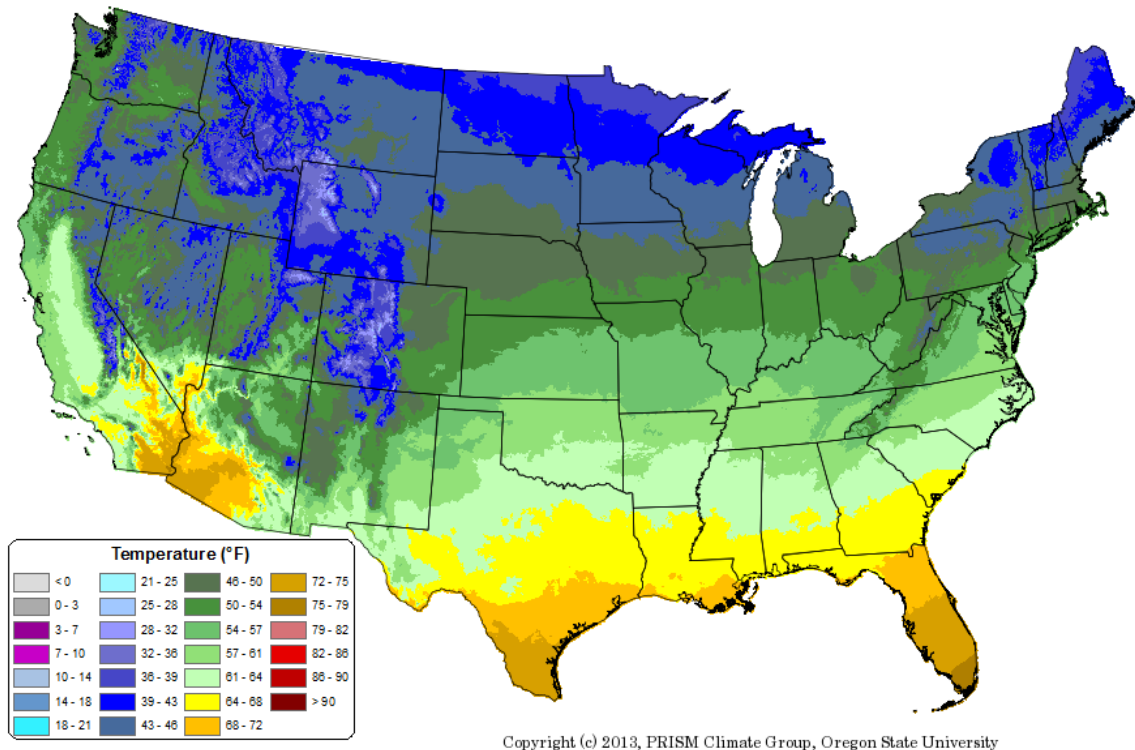
Figure 6 Normal mean temperature from 1981 to 2010 (Data compiled from PRISM Climate Group source: http://www.prism.oregonstate.edu/)
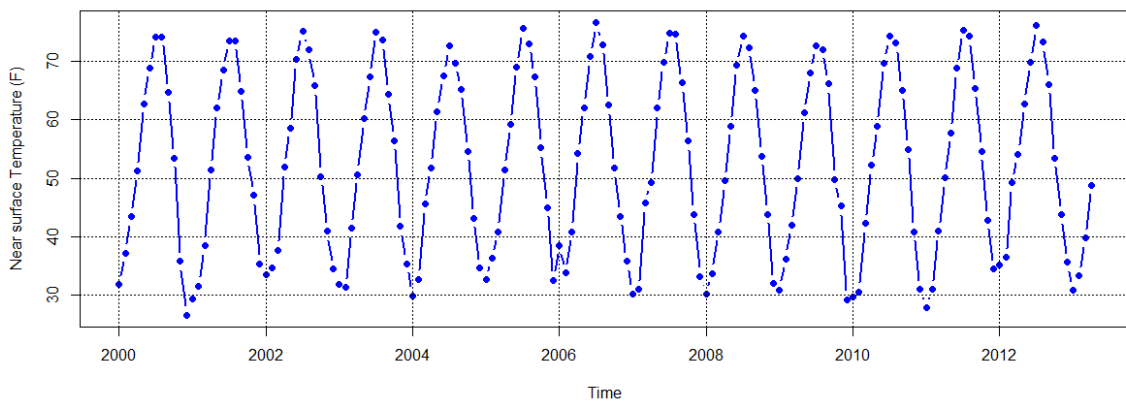
Figure 7 Spatial mean monthly near surface air temperature over CONUS from 2003 to 2013

Land use /Land cover

The major uses in US were forest-use land, 651 million acres, about 28.8 percent; grassland pasture and range land, 587 million acres, about 25.9 percent; cropland, 442 million acres, 19.5 percent and urban land, 60 million acres, about 2.6 percent (*ERS*, 2002). Figure 8 shows the fraction of land cover that is classified as agriculture. The major agriculture lands are located in the Great Plain, especially in Iowa, Illinois, South Dakota, North Dakota and Minnesota. The fraction of agriculture are higher than 0.7. Agriculture has been the life force of the Great Plain economy, therefore, agricultural drought has significant impact on the life in these areas. The eastern US has less agricultural land (<0.3), and also in the west.
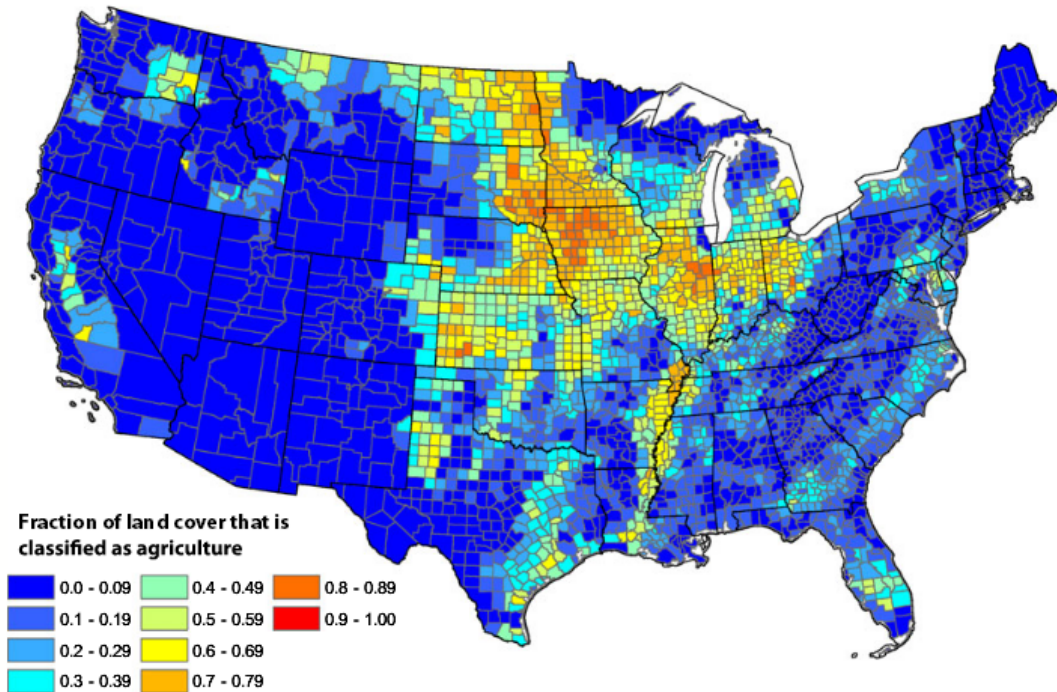
Figure 8 Fraction of land cover that is classified as agriculture over the CONUS (*ERS*, 2002)

Data

GRACE

Specific to the goals of this project, GRACE data were used to extract estimates of terrestrial water storage (TWS). In this study, monthly GRACE TWS data covering the time periods from April 2003 to August 2012 were downloaded from the NASA Jet Propulsion Laboratory website. The GRACE TWS anomaly ranges from -75 cm to 95cm during the study period and the change of TWS between two neighboring month ranges from -66 cm to 56 cm.

NOAH Land Surface Model

For agricultural purposes, soil moisture is the key indicator as such agricultural drought indices are often based on soil moisture deficit analysis. In situ measurement is the most accurate way to obtain soil moisture, but it is point based and is impossible to be used for large scaled soil moisture monitoring. Therefore, soil moisture simulated by NOAH LSM was used to calculate SMDI. NOAH data for this study was downloaded from the NASA Giovanni website, at a 1° by 1° resolution on a monthly basis starting in April 2003 until August 2012. NOAH LSM provides soil moisture simulations at four layers: 0-0.1m, 0.1-0.4m, 0.4-1m, and 1-2m). In this study, we focus on the entire 2 meters soil layer, because the vegetation root zone is usually ranging from 10 cm to several meters. The native format of the monthly NOAH data preserved the individual soil moisture layers, snow water equivalent, and canopy storage. In this study, each of these layers was summed into a single soil moisture value for each grid point. In order to be comparable with GRACE TWS, NOAH soil moisture was deviated by data form 2005 to 2009. NOAH soil moisture values range from -34 cm to 74 cm, and the monthly soil

moisture change between the range from -46 cm to 30cm in the study period.

PRISM precipitation

We used precipitation data from Parameter-elevation Regressions on Independent Slopes Model (PRISM), which was recognized as the highest-quality spatial climate data developed by PRISM Climate Group (*Daly et al.*, 2008). The PRSIM precipitation contains monthly precipitation over the CONUS since January 1895 with spatial resolutions of 800m, 2 km and 4 km based on point observations. In this study, the precipitation data was aggregated to 1°×1° grid by taking the average precipitation values.

MOD16 evapotranspiration (ET)

The MODIS was operated on both Terra and Aqua platforms with a viewing swath width of 2,330 km. The MODIS instrument provides data of the earth surface every one to two days and the spatial resolutions are 250m, 500m and 1000m for different bands. Used in this study, the MODIS MOD 16 evapotranspiration is a NASA/EOS project to estimate the land surface evapotranspiration based on MODIS and global meteorology data. This dataset provides transpiration by vegetation and also evaporation from soil and canopy (*Mu et al.*, 2011). The MOD16 ET with a spatial resolution of 0.5° was aggregated to 1°×1° grid by taking the average values.

US Drought Monitor (USDM)

In this study USDM was used as a reference to evaluate the performance of SMDI over the CONUS. In 1998 the National Drought Mitigation Center (NDMC) and the National Oceanic and Atmospheric Administration's Climate Prediction Center

(NOAA/CPC) started a program to improve drought monitoring and named their products USDM over the United States. USDM is developed based on in-situ measurement and remote sensing products. The USDM combined much information that impact water budget including climate and hydrological processes (Table 2). The main parameters used in this product are the PDSI, Climate Prediction Center (CPC) Soil Moisture Model, USGS Daily Stream flow, Percent of Normal Precipitation, SPI and Satellite Vegetation Health Index. US drought monitor has been widely used as a reference to evaluate the ability of different drought indices. For example Rhee et al (2010) used US drought monitor maps to assess an agricultural drought index Scaled Drought Condition Index (SDCI). The US drought monitor classified drought on a scale from D0 (abnormally dry) to D4 (exceptional drought). The details of the drought categories are listed in Table 2.

Table 2 The association of the six key objective drought indication (including Palmer drought index, CPC soil moisture, USGS weekly stream flow, percent of normal precipitation, SPI and satellite vegetation index with the magnitude of drought severity in the drought monitor (http://droughtmonitor.unl.edu/classify.htm).

Category	Description	Palmer Drought Index	CPC Soil moisture (Percentiles)
D0	Abnormally dry	-1.0 to -1.9	21-30
D1	Moderate drought	-2.0 to -2.9	11-20
D2	Severe drought	-3.0 to -3.9	6-10
D3	Extreme drought	-4.0 to -4.9	3-5
D4	Exceptional Drought	-5.0 or less	0-2

USGS weekly stream flow (Percentiles)	Percent of normal precipitation	Standardized Precipitation Index	Satellite vegetation
21-30	<75% for 3 months	-0.5 to -0.7	36-45
11-20	<70% for 3 months	-0.8 to -1.2	26-35
6-10	<65% for 6 months	-1.3 to -1.5	16-25
3-5	<60% for 6 months	-1.6 to -1.9	6-15
0-2	<65% for 12 months	-2.0 or less	1-5

CHAPTER IV

METHODOLOGY

Agricultural drought monitoring

Drought is a continuous phenomenon that is influenced by the dry or wet conditions from previous months (*Palmer*, 1965). SMDI (*Narasimhan and Srinivasan*, 2005) was calculated by combining the current soil moisture deficit (*SMD*) and the previous months SMDI using different weights. SMDI like PDSI, is a monthly accumulation index, which combines the data on the soil *SMD* from the previous months in the following recursion:

$$
\begin{aligned}
SMDI_t &= p \times SMDI_{t-1} + q \times SMD_t \qquad t \geq 2 \\
SMDI_t &= SMD_t / 50 \qquad\qquad\qquad\quad t = 1
\end{aligned}
\tag{2}
$$

Following the *Narasimhan and Srinivasan* (2005), *SMD* of the current month is estimated as:

$$
\begin{aligned}
SMD_t &= \frac{SM_t - MSM_j}{MSM_j - \min SM_j} \times 100 \qquad SM_t \leq MSM_j \\
SMD_t &= \frac{SM_t - MSM_j}{\max SM_j - MSM_j} \times 100 \qquad SM_t > MSM_j
\end{aligned}
\tag{3}
$$

Where $SMD_{i,j}$ (%) is the soil moisture deficit of one particular month t. where SM (cm), MSM (cm), maxSM (cm), and minSM (cm) represent monthly soil moisture, the climatological median monthly soil moisture, and the climatological maximum and

minimum monthly soil moisture, respectively. Subscript n (= 1…12) denotes the month that t currently represents. For example, if t represents April 2005, then n is 4. The *SMD* values (in percentage) vary from -100, an extremely dry condition, to 100, an extremely wet condition. Eq. (3) removes the seasonal dependence in soil moisture, resulting in *SMD* values comparable across seasons. These *SMD* values inform the dryness and wetness for each particular month, relative to historical conditions.

Duration factors (p and q) indicate the sensitivity of the drought index to moisture conditions of the previous month and to the current water storage deficit: high values of p render *SMDI* less sensitive to the weather of current month (e.g., heavy rains) (*Wells et al.*, 2004), and high values of q indicate that *SMDI* is more sensitive to the current soil moisture deficit.

p and q can be computed by using Eq. (4) and (5) (*Wells et al.*, 2004):

$$p = 1 - \frac{m}{m+b} \qquad (4)$$

$$q = \frac{C}{m+b} \qquad (5)$$

where m and b are the slope and intercept of the linear regression between the cumulative *SMD* in driest and wettest conditions vs different durations from one month to eighteen months (Figure 9). For each grid cell, to evaluate m and b in dry conditions, the driest month in the history (lowest SMD) was first selected and plotted for one-month duration. Then the running sums of *SMD* for every two neighboring months were calculated and the lowest cumulative *SMD* was selected as well for two-month duration. Same process repeated until eighteen-month duration and highest cumulative *SMD* was chosen for wet conditions. Then a linear regression was used to fit these plots and identify the slope, $-m$

and intercept, *b*. *C* is from the best-fit line of a drought monograph to scale, which ranges from -100 to 100 which is then scaled to fit the range of PDSI categories (-4 – 4).

Accumulated indexof various lengths
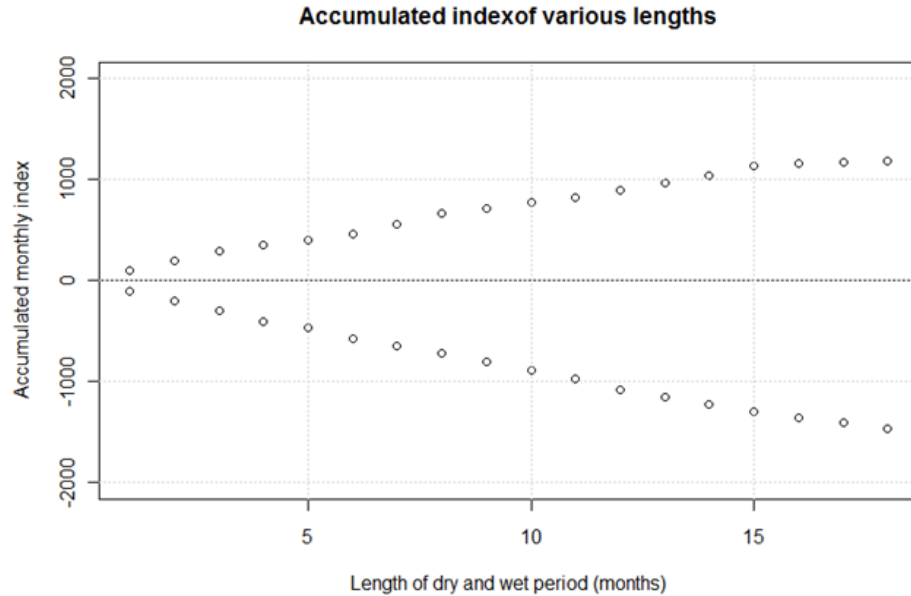
Figure 9 An example of the calculation of m (slope) and b (intercept).

Agricultural drought prediction

Previous studies (e.g. *Narasimhan and Srinivasan*, 2005) show that the SMDI can be used as a proxy for agricultural drought. Therefore, drought prediction can be achieved by estimating SMDI values at a future time. Eqs. (2) and (3) imply that SM_{t+1}, the soil moisture value for month *t*+1, is a key variable needed for predicting $SMDI_{t+1}$. SM_{t+1} can be calculated using Eq. (6):

$$SM_{t+1} = SM_t + \Delta\theta_{t+1} \quad (6)$$

where $\Delta\theta_{t+1}$ represents the change in soil moisture between *t* and *t*+1. Soil moisture change ($\Delta\theta$) reflects net mass balance of different hydrological processes including precipitation, evapotranspiration, runoff, and interactions between the unsaturated zone and groundwater.

Studies have shown that soil moisture responses, often with a lag, to the climatic forcing. For example, Sheffield et al (2004) found a one month lag between atmospheric conditions and soil moisture during the 1988 drought in the US. Luo and Wood (2007) showed high correlation between averaged precipitation in January, February and March 2007 and soil moisture percentiles in March 2007 over the CONUS (Figure 10). In addition, as a source of soil water content, groundwater storage deficit will also result in surface soil moisture decline, especially in the areas where the ground water table is close to surface (*Chen and Hu*, 2004). Since *TWS* not only measures water storage in the land surface and unsaturated zone but also ground water. We try to include TWS in the MLR model as well.
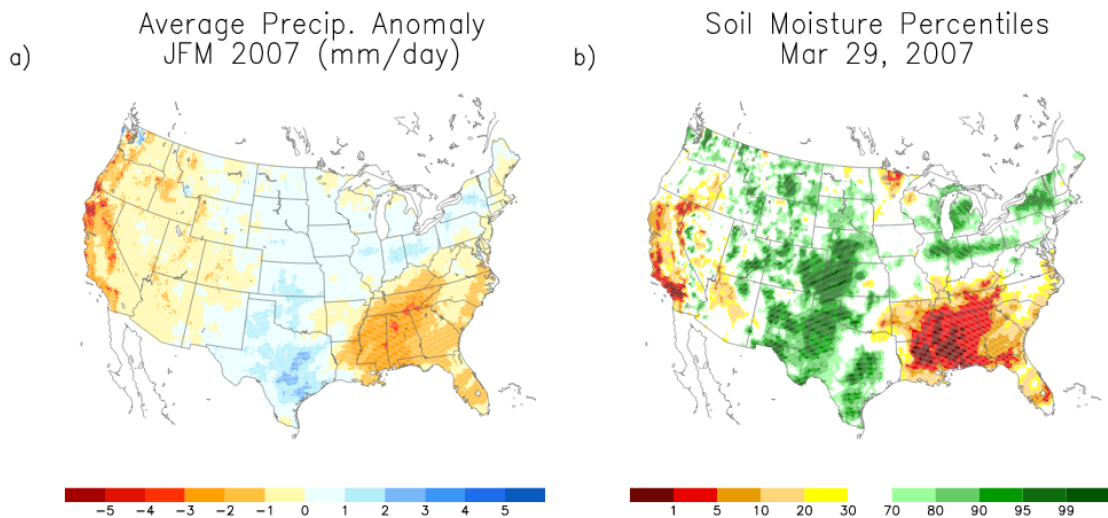
Figure 10 Mean precipitation (mm/day) anomaly against time period from 1949 to 2004, for JFM 2007 (a) and the soil moisture percentiles on March 29, 2007 (b) (*Luo and Wood*, 2007)

Therefore, a MLR model was applied to estimate soil moisture change using the hydrological and climatic variables at previous months that affect or constrain soil moisture changes.

$$
\begin{aligned}
\Delta\theta_{j,t+1} = a_1 \times P_{j,t} + a_2 \times P_{j,t-1} + b_1 \times ET_{j,t} + b_2 \times ET_{j,t-1} + c_1 \times \Delta TWS_{j,t} + c_2 \times \Delta TWS_{j,t-1} \\
+ d \times \text{season}_{t+1,} + \sum e_i \times \text{watershed}_i + \varepsilon_{j,t+1}
\end{aligned}
\tag{7}
$$

where $\Delta\theta$ *is* the soil moisture difference between t and $t+1$, for grid j, in watershed i. a, b, c, d and e are coefficients to be determined for precipitation (P), evapotranspiration (ET), change of terrestrial water storage (ΔTWS), seasonality and watersheds, respectively; and ε_{t+1} is the error term of the model. Among the hydrologic variables that directly affect the soil moisture content, P, ET and ΔTWS are routinely observed. Figure 11 shows the average monthly variations of four hydrological variables, $\Delta\theta$, P, ET and ΔTWS, over the CONUS. Clearly, all the four variables exhibit seasonality, even though ET peaks during summer whereas $\Delta\theta$ and ΔTWS peak during winter. To account for the seasonality in the model, we denote spring (March to May) as 1, summer (June to August) 2, fall (September to November) 3, and winter (December to February) 4. We also tested four dummy variables to represent seasons, but all the four coefficients are not significant. Due to the spatial variance, the impact of climatic forcing and groundwater to soil moisture change are different (Table 3). For example, in most of the regions, such as in Pacific Northwest Region, California Region and Lower Colorado Region, precipitation at month t has positive correlation with soil moisture change at month $t+1$, which indicates soil water supplement from precipitation. However, in other regions, such as Upper Mississippi Region, Missouri Region and Souris-Red-Rainy Region, there are no correlations or even negative correlation between them. The large correlation coefficient differences are also found for other variables. To account for regional differences, we

included 18 dummy variables to represent for the 18 individual watersheds (Figure 12), following the USGS (*USGS*, 2013). The reason that we use watersheds to indicate regional differences is because a watershed likes a precipitation collector, and water drops into the same watershed converges to the same outlet in the form of surface and subsurface runoff. Therefore, seasonal and regional terms provide a constraint on runoff, which is not readily available at the 1°×1° scale and therefore not directly expressed in the model.
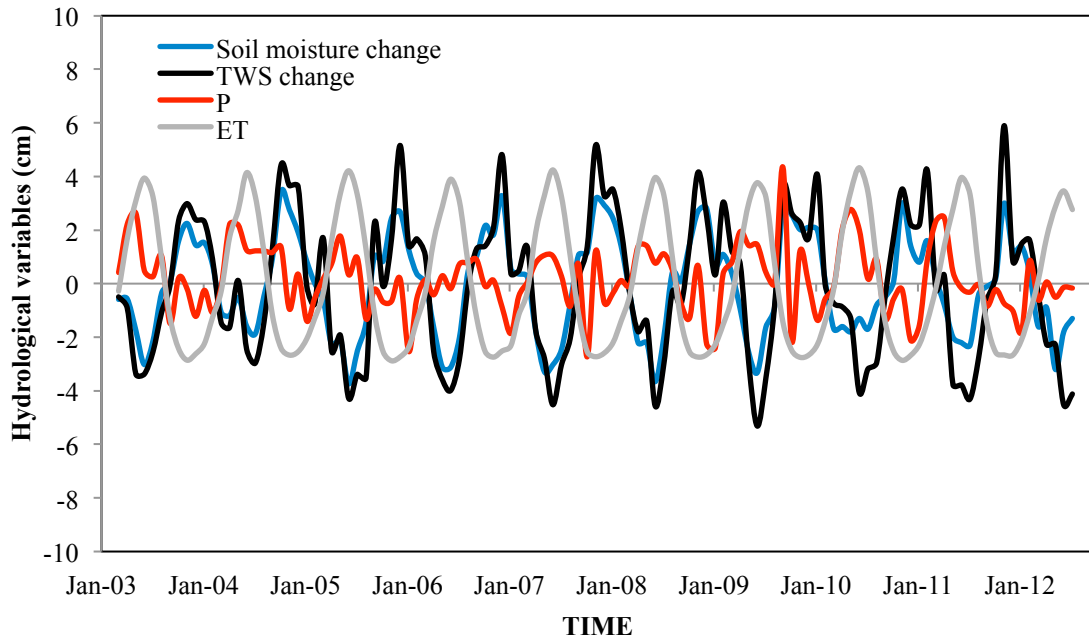
Figure 11 Temporal variations in change of soil moisture, change of TWS, precipitation and ET averaged over the CONUS.

Table 3. Correlation matrix for soil moisture change at month $t+1$ and P, ET, ΔTWS at month t and t-1.

	REG_NAME	P_t	P_{t-1}	ET_t	ET_{t-1}	ΔTWS_t	ΔTWS_{t-1}
1	Upper Mississippi Region	-0.068	-0.148	-0.556	-0.407	0.285	0.186
2	Upper Colorado Region	0.201	0.141	-0.368	-0.284	0.388	0.271
3	Arkansas-White-Red Region	0.094	-0.041	-0.360	-0.282	0.386	0.317
4	California Region	0.335	0.181	-0.623	-0.539	0.429	0.354
5	Texas-Gulf Region	0.182	0.044	-0.193	-0.138	0.268	0.242

Table 3 cont.

6	Great Basin Region	0.241	0.115	-0.368	-0.338	0.447	0.317
7	Great Lakes Region	0.026	-0.043	-0.448	-0.314	0.290	0.164
8	Tennessee Region	0.069	-0.068	-0.529	-0.391	0.467	0.347
9	Lower Colorado Region	0.296	0.163	-0.096	-0.072	0.258	0.224
10	Lower Mississippi Region	0.133	-0.035	-0.484	-0.368	0.302	0.218
11	Mid Atlantic Region	0.070	0.020	-0.448	-0.288	0.471	0.389
12	Missouri Region	-0.120	-0.254	-0.501	-0.385	0.301	0.197
13	New England Region	0.046	-0.031	-0.326	-0.160	0.405	0.357
14	Ohio Region	0.014	-0.066	-0.571	-0.422	0.549	0.458
15	Pacific Northwest Region	0.324	0.211	-0.589	-0.451	0.510	0.406
16	Rio Grande Region	0.245	0.135	0.132	0.127	0.091	0.051
17	Souris-Red-Rainy Region	-0.098	-0.254	-0.511	-0.336	0.080	0.034
18	South Atlantic-Gulf Region	0.155	0.023	-0.239	-0.152	0.153	0.103

Figure 12 Distribution of 18 watersheds in the CONUS by USGS (*USGS*, 2013)

The reason that we chose *ET*, *ΔTWS*, and *P* values at both *t* and *t*-1 months as explanatory variables is well illustrated in Figure 13, which shows the auto-correlation of *P*, *ET* and *ΔTWS* in seven major watersheds of the CONUS. The autocorrelations for the

three variables change from positive to negative all at approximately three-month lag, indicating a clear seasonal pattern. This pattern, while exhibits some regional variability, is largely consistent throughout all the major watersheds in the CONUS.
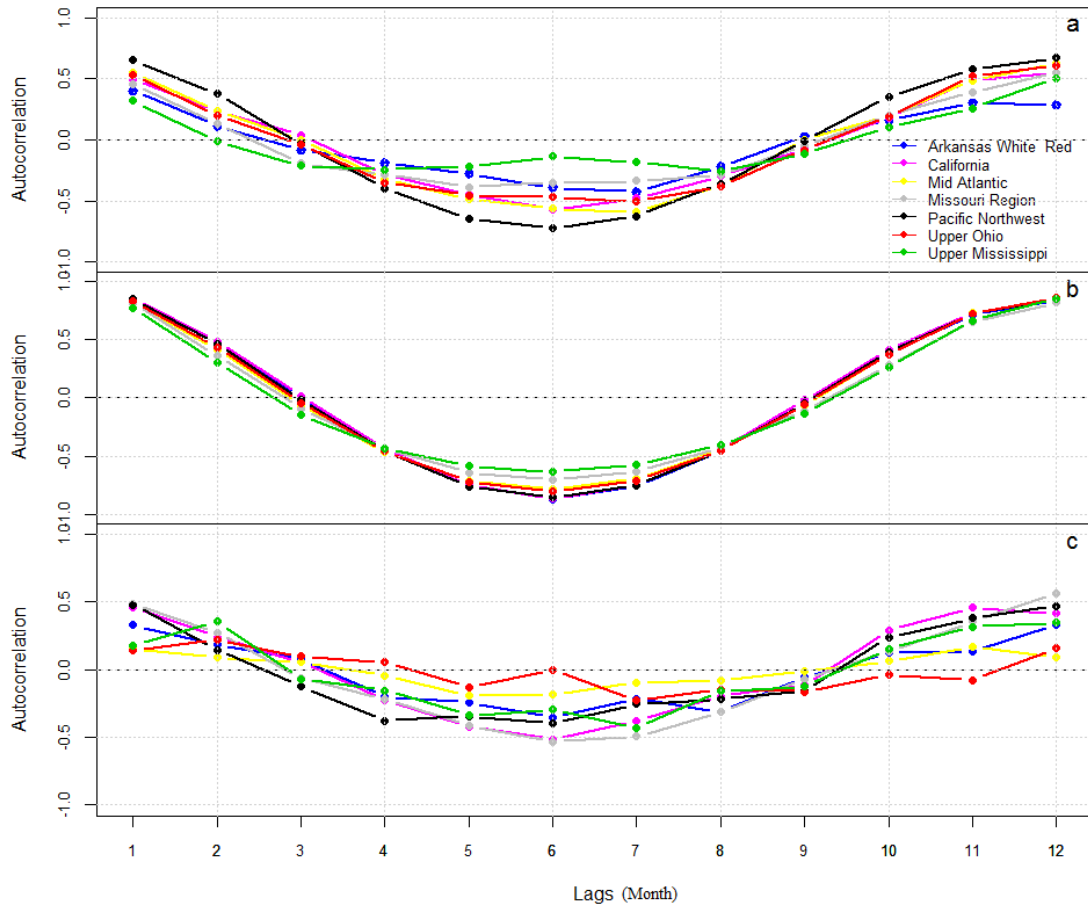
Figure 13. Autocorrelation analyses of TWS (a), ET (b) and precipitation (c) over seven major watersheds in the CONUS from 2003 to 2009.

The models were judged by adjusted R^2 and Mean absolute error (MAE). The adjusted R^2 is a measure of goodness-of-fit of the models based on the coefficient of determination R^2, and is able to compare the models with different input variables. Adjusted R^2 is estimated by:

$$\bar{R}^2 = 1 - \frac{(N-1)}{(N-K-1)}(1 - R^2) \quad (8)$$

where N is the number of observations, K is the number of input variables.

The MAE measures the bias and precision of the models. It calculates the absolute differences of the observed and simulated value (*Willmott*, 1981). The MAE is nonnegative and small MAE indicates high precision and is given by:

$$MAE = N^{-1} \sum |O_{j,t+1} - P_{j,t+1}| \quad (9)$$

Where N is the number of observations, $O_{j,t+1}$ and $P_{j,t+1}$ are the observed and predicted soil moisture change value at grid j, time $t+1$.

Then the estimated soil moisture change was applied to Eq. 2,3 and 4 to obtain $SMDI_{t+1}$.

In this study, drought prediction was also calculated for two- to six- month lead. Same method was applied to estimate the coefficients of the variables. For example, to estimate soil moisture change at $t+2$, Eq (10) is used:

$$\Delta\theta_{j,t+2} = a_1 \times P_{j,t} + a_2 \times P_{j,t-1} + b_1 \times ET_{j,t} + b_2 \times ET_{j,t-1} + c_1 \times \Delta TWS_{j,t} + c_2 \times \Delta TWS_{j,t-1} \\ + d \times season_{t+2} + \sum e_i \times watershed_i + \varepsilon_{t+2,j} \quad (10)$$

Then the predicted soil moisture change at month $t+2$ was applied to $SMDI_{t+2}$ prediction. Similar to the method described in drought monitoring, the $SMDI_{t+2}$ was calculated by following equations:

$$SM_{t+2} = SM_t + \Delta\theta_{t+1} + \Delta\theta_{t+2} \quad (11)$$

$$SMD_{t+2} = \frac{SM_{t+2} - MSM_{j+2}}{MSM_{j+2} - \min SM_{j+2}} \times 100 \qquad SM_{t+2} \le MSM_{j+2}$$

$$SMD_{t+2} = \frac{SM_{t+2} - MSM_{j+2}}{\max SM_{j+2} - MSM_{j+2}} \times 100 \qquad SM_{t+2} > MSM_{j+2}$$

$$(12)$$

$$SMDI_{t+2} = p \times SMDI_{t+1} + q \times SMD_{t+2} \quad (13)$$

Same method was applied to calculate SMDI at lead time from three to six months.

CHAPTER V

RESULTS

Agricultural drought monitoring

In this section, SMDI is used to monitor drought evolution on large scale. In order to identify the reliability of the drought index, the SMDI is compared with a widely used drought index, USDM, and both the temporal change and the spatial distributions of current 2010-2012 drought event are discussed.

Temporal variability of drought severity

The fractional areas of the CONUS in drought from SMDI and the USDM from 2003 to 2012 were compared to estimate the performance of SMDI on drought monitoring on large scale. Although we cannot directly compare the two results because USDM is based on drought indices including information not only from soil moisture but climatic and hydrological variables like precipitation, temperature and stream flows (*Heim* 2002; *Svoboda et al.*, 2002). The categories of the two results are also different (Table 2). Clearly, the drought affected areas based on USDM (Figure 14 b) are consistently greater than the estimates based on SMDI (Figure 14 a), which is expected given that the former covers a wider range of drought conditions (meteorological, agricultural and hydrological drought) than the latter (agricultural drought only). Despite this difference, both indices show very similar temporal pattern (Figure 14). As for the

study period from 2003 to 2012, both of them indicated three major drought events, 2003 to 2004, 2006 to 2008 and 2010 to 2012, respectively. The most recent severe drought in

the United States initiated in late 2010. Both drought monitoring indices indicate that the area affected by drought in the CONUS increased sharply in winter 2010 and spring 2011, with about 30% of entire CONUS under moderate/severe drought conditions. In 2012, the affected regions continued increasing after a decline in spring and reached over 60% in summer.
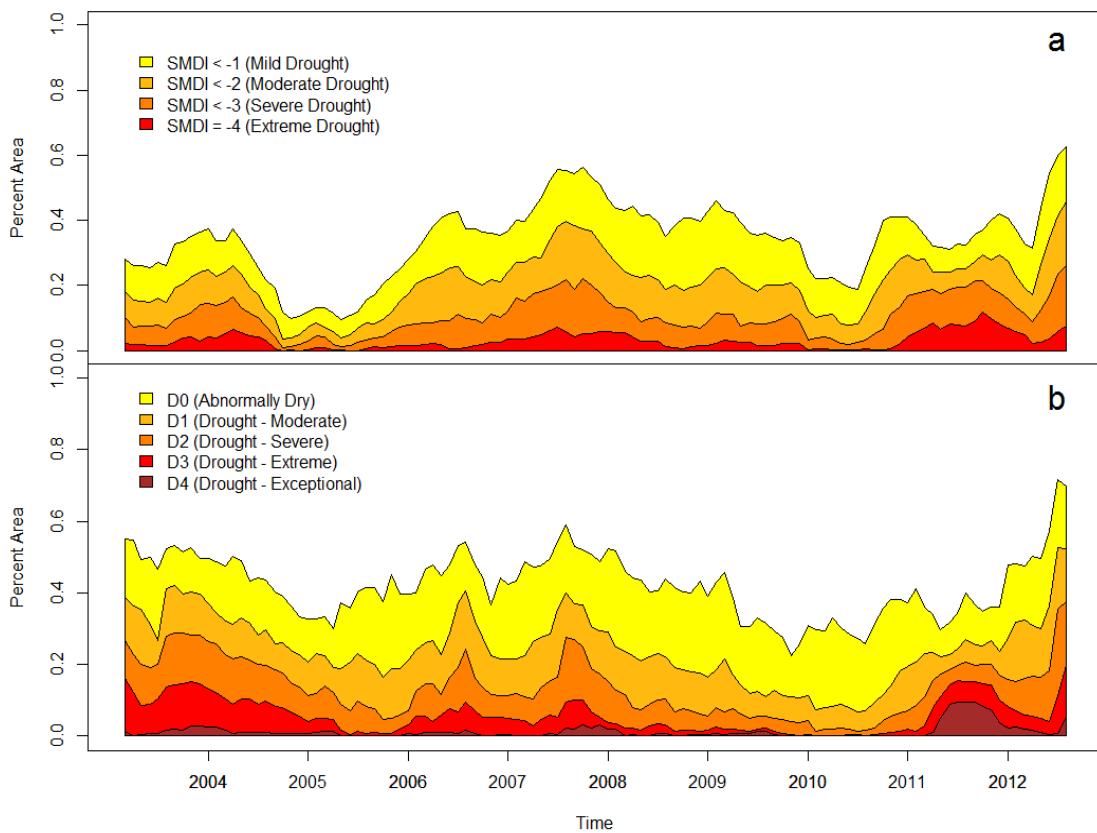
Figure 14 Time series of fractional area over the CONUS from US drought monitor (a) from January 2000 to January 2013 and SMDI (b) from January 2003 to August 2012.

Spatial evaluation of SMDI in monitoring 2010 to 2012 drought

In addition to the temporal evaluation, the spatial evolution of drought in the last two years based on SMDI and USDM were compared. The USDM provides weekly drought observation maps and the ones in Figure 15 are the drought observations of the last week of every month from January 2010 to August 2012. We compared the drought conditions from 2003 to 2012 and the two products show a similar spatial pattern in every month, in this section, we only show the maps of the most recent drought event from 2010 to 2012. Since drought conditions are quite continuous, the spatial pattern changes in one month are not significant. The maps for the last week of one month are representative to the corresponding month.

The CONUS was characterized by wet condition in early 2010 (Figure 15). Only some abnormal dry conditions were recorded in the western areas. From the USDM, the 2010 to 2012 drought started first in winter 2010 in the southern US including Texas and part of Louisiana, Mississippi, Florida, and Alabama. SMDI also indicates the drought occurrence in the same area in winter 2010. The SMDI classified the drought severity in the southern US as extreme drought, while the USDM characterized it as moderate drought. The difference indicates that the drought severity at the end of 2010 in southern US had higher impact on agriculture than other aspects. The drought then expanded and gradually covered the whole Arizona, New- Mexico, Texas and Georgia areas and the drought became more severe later in summer. The spatial and temporal evolution of SMDI coincides with the USDM results and indicates an extreme drought event in the southern US The 2011 summer drought was reported as the driest year since 1895 (*Fannin*, 2012). The successful evaluation of this extreme drought proves SMDI having

ability to monitor extreme drought conditions. In spring 2012, both SMDI and US drought monitor indicate a drought relief in the southern regions, because precipitation over those states returned to normal in spring 2012. However, the precipitation did not recover the drought, and areas affected by drought expended to almost the entire CONUS in summer 2012. Compared with the US drought monitor, SMDI monitoring well evaluates the extreme condition in the entire US although it underestimates the drought severity in Oklahoma. Compared with USDM, more extreme conditions were shown from SMDI. The reason could be that we denote the driest time period from 2003 to 2012 as extreme drought. However, ten years soil moisture conditions are not representative to long term variations, and more extreme condition may occur in the past drought events. The USDM products are based on the weather conditions over the past century. However, generally, SMDI can still well evaluate the drought evolution of the 2010 to 2012 drought especially the worst drought event in southern US of the century.
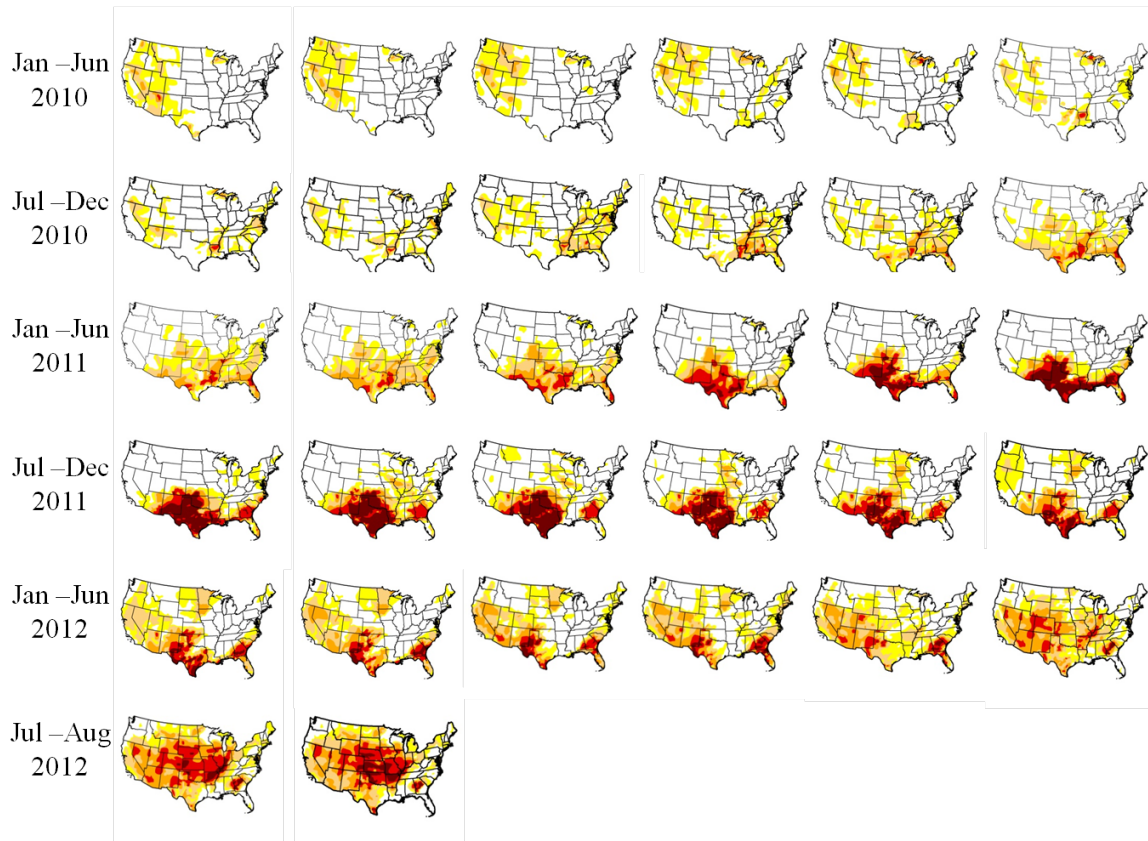
Figure 15. 2010 to 2012 drought evolution maps from USDM and the maps in the figure are
drought conditions for the last week of the month). Red means dry and dark color means severe
drought. White means normal or wet conditions.
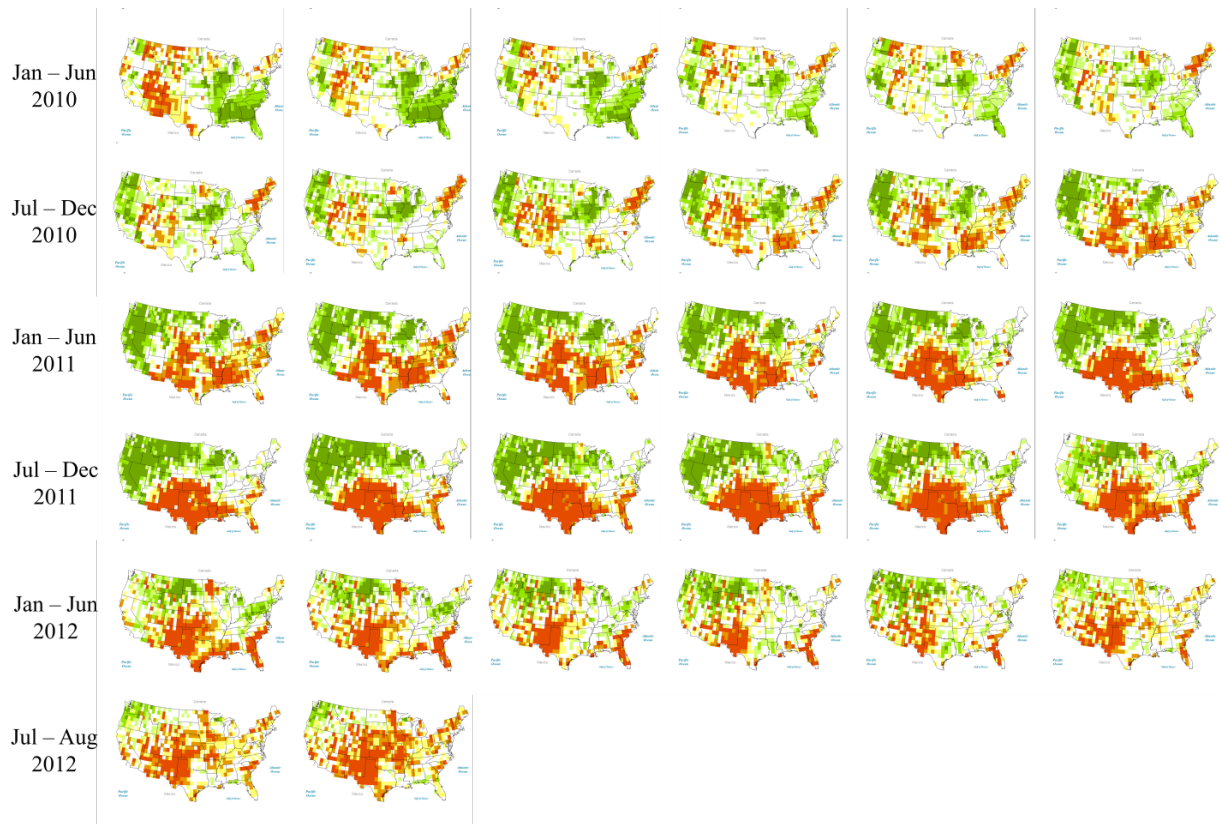
Figure 16. Current drought evolution from SMDI from January 2010 to August 2012 (greenish color indicates wet conditions and the yellowish color means dry)

Agricultural drought prediction

MLR stability analysis

For agricultural drought prediction, MLR model was applied to estimate the relation between soil moisture change and the predictors such as P, ET, and ΔTWS.

First we evaluated the stability of the MLR model. The training data were further divided into subsets with progressively shortened durations. For example, the MLR analysis was performed first with the entire training set, and then with the subsets of 6-year spans (2003-2008 and 2004-2009). The process was repeated all the way to subsets of a 1-year span.

Table 4 lists the coefficients of the MLR model (Eq. 6) estimated using different training datasets. All the estimated coefficients are statistically significant. For each coefficient, its relative standard deviations (RSD) across all the training sets were estimated as the ratio of the standard deviation to the average. The RSD values are < 15% for all the coefficients (except for c_2), indicating that the coefficients are numerically stable and the statistical specification is robust. Even though c_2 has the highest RSD value of 45%, its mean value is only 0.054, indicating that the soil moisture change is not very sensitive to ΔTWS at two-month lead. As can be expected, the ΔTWS and P values at the current month (t) have positive and ET has negative contributions to soil moisture changes. Counter-intuitively, P and ET at the t-1 month have opposite contributions to soil moisture changes at t+1 month. This pattern is consistent regardless of which training set was used. One possible reason could be the strong auto-correlation exhibited by P and ET at a one-month lag (Figure 13). Still, as discussed below, it is necessary to include P and ET values at both t and t-1 months as the predictors. The coefficient d associated with

seasonality has a mean value of ~0.5 (>0), indicating a general trend that soil moisture tends to increase/accumulate during winter and decrease during spring and summer, which is consistent with Figure 11.

Table 4. Comparison of the MLR model (Eq. (6)) developed using different training sets. With each training set, the mean value and the standard deviation (in parentheses) for each explanatory varaible, as well as the evaluations of the model in terms of adjusted-R^2 and mean absolute error (MAE), are shown. The last three rows show the mean, standard deviation (SD), and relative standard deviation (RSD) of each coefficient over the entire trainings.

	a_1	a_2	b_1	b_2	c1	c2	d1	Adj-R^2	MAE
2003 - 2004	0.140 (0.006)	-0.096 (0.006)	-0.716 (0.016)	0.482 (0.016)	0.086 (0.008)	0.022 (0.007)	0.387 (0.038)	0.39	1.8
2003 - 2005	0.174 (0.004)	-0.157 (0.004)	-0.695 (0.011)	0.575 (0.011)	0.124 (0.005)	0.043 (0.005)	0.351 (0.021)	0.39	1.8
2003 - 2006	0.177 (0.003)	-0.148 (0.003)	-0.747 (0.009)	0.568 (0.009)	0.100 (0.004)	0.057 (0.004)	0.443 (0.017)	0.40	1.9
2003 - 2007	0.179 (0.003)	-0.157 (0.003)	-0.734 (0.008)	0.601 (0.008)	0.116 (0.004)	0.059 (0.004)	0.496 (0.014)	0.40	1.9
2003 - 2008	0.172 (0.003)	-0.146 (0.003)	-0.796 (0.007)	0.598 (0.007)	0.113 (0.003)	0.056 (0.003)	0.479 (0.013)	0.42	1.9
2003 - 2009	**0.173** (0.002)	**-0.149** (0.002)	**-0.778** (0.007)	**0.621** (0.007)	**0.123** (0.003)	**0.056** (0.003)	**0.525** (0.012)	**0.41**	**1.9**
2004 - 2005	0.179 (0.005)	-0.197 (0.005)	-0.760 (0.016)	0.605 (0.016)	0.149 (0.007)	0.047 (0.007)	0.508 (0.038)	0.44	1.7
2004 - 2006	0.186 (0.004)	-0.164 (0.004)	-0.749 (0.012)	0.624 (0.011)	0.115 (0.005)	0.074 (0.005)	0.478 (0.023)	0.41	1.9
2004 - 2007	0.184 (0.003)	-0.169 (0.003)	-0.773 (0.010)	0.607 (0.009)	0.115 (0.004)	0.056 (0.004)	0.489 (0.017)	0.42	1.9
2004 - 2008	0.178 (0.003)	-0.156 (0.003)	-0.791 (0.008)	0.648 (0.008)	0.132 (0.004)	0.073 (0.004)	0.519 (0.015)	0.43	2.0
2004 - 2009	0.174 (0.003)	-0.154 (0.003)	-0.827 (0.008)	0.615 (0.008)	0.117 (0.004)	0.047 (0.004)	0.512 (0.013)	0.42	2.0
2005 - 2006	0.164 (0.006)	-0.149 (0.006)	-0.728 (0.017)	0.573 (0.017)	0.085 (0.009)	0.097 (0.008)	0.718 (0.040)	0.39	2.1

Table 4 cont.

2005 - 2007	0.181 (0.004)	-0.152 (0.004)	-0.784 (0.012)	0.559 (0.012)	0.098 (0.006)	0.048 (0.006)	0.551 (0.022)	0.38	2.0
2005 - 2008	0.164 (0.003)	-0.147 (0.003)	-0.795 (0.010)	0.640 (0.010)	0.136 (0.005)	0.082 (0.005)	0.573 (0.018)	0.39	2.0
2005 - 2009	0.167 (0.003)	-0.142 (0.003)	-0.845 (0.009)	0.593 (0.009)	0.110 (0.004)	0.040 (0.004)	0.544 (0.015)	0.40	2.0
2006 - 2007	0.172 (0.006)	-0.167 (0.006)	-0.826 (0.017)	0.631 (0.016)	0.120 (0.009)	0.013 (0.008)	0.556 (0.038)	0.43	1.8
2006 - 2008	0.162 (0.004)	-0.136 (0.004)	-0.852 (0.012)	0.688 (0.012)	0.154 (0.006)	0.070 (0.006)	0.535 (0.023)	0.38	2.0
2006 - 2009	0.161 (0.003)	-0.143 (0.003)	-0.876 (0.010)	0.631 (0.010)	0.127 (0.005)	0.031 (0.005)	0.533 (0.018)	0.39	2.0
2007 - 2008	0.147 (0.006)	-0.110 (0.006)	-0.922 (0.017)	0.744 (0.017)	0.143 (0.009)	0.116 (0.009)	0.665 (0.040)	0.38	2.1
2007 - 2009	0.158 (0.004)	-0.129 (0.004)	-0.912 (0.013)	0.623 (0.013)	0.112 (0.006)	0.031 (0.006)	0.582 (0.023)	0.39	2.1
2008 - 2009	0.160 (0.007)	-0.129 (0.007)	-0.847 (0.019)	0.617 (0.018)	0.121 (0.009)	0.025 (0.009)	0.469 (0.042)	0.41	2.1
mean	**0.169**	**-0.147**	**-0.798**	**0.612**	**0.119**	**0.054**	**0.496**		
STD	**0.012**	**0.020**	**0.061**	**0.050**	**0.018**	**0.024**	**0.134**		
RSD	**7%**	**-14%**	**-8%**	**8%**	**15%**	**45%**	**15%**		

The goodness of fit of the MLR models developed using different training sets is evaluated using adjusted R^2 and mean absolute error (MAE) (Table 4). The values of adjusted R^2 and MAE varied little among different trainings, with a mean value of 0.4 and 2 cm, respectively. Again, this indicates that the model in general is robust. For prediction, we simply used the model estimated from the entire testing period from 2003 to 2009 to estimate change of soil moisture:

$$\Delta\theta_{t+1} = 0.173 \times P_t - 0.149 \times P_{t-1} - 0.796 \times ET_t + 0.598 \times ET_{t-1} + 0.113 \times \Delta TWS_t + 0.056 \times \Delta TWS_t \\ + 0.525 \times season \tag{14}$$

The coefficients for the 18 dummy watershed variables varied from -1.2 to -0.5 and for clarity, are not shown in the equation.

The MLR model is stable when using data in different time spans from 2003 to 2009 as inputs. The coefficients of the explanatory variables are consistent with RSD lower than 15%. Since all of the factors contribute to the soil moisture change, we evaluated the relative importance of each component in affecting the soil moisture deficit. Among the three components used in MLR, *ET* is the most significant variable that influences soil moisture change and adjusted R^2 increased 50%. The contributions of precipitation and TWS are less, both of the two variables result in only about a 7% improvement of the model performance. Houborg et al (2012) also found that incorporating of the GRACE TWS data into their Catchment Land Surface Model does not improve the estimation of soil moisture significantly. The reason could be that monthly GRACE TWS which includes groundwater varies slowly while soil moisture responds quickly to atmospheric forcing.

Due to the high autocorrelation of *P* and *ET,* the contribution at one- and two-months are opposite. However using predictors at two lead time as well is necessary.

Table 5 shows MLR model using components at one month lead only. Compared with table 4, the adjusted R^2 decreased significantly as well as the magnitudes of the coefficient for all time spans. MAE increased to higher than 2 cm. Therefore using predictors at one- and two- month lead times can better estimate the change of soil moisture.

Table 5 The same as Table 4, but *P*, *ET*, ΔTWS at one month lead were used in the MLR model.

	a	b	c	d	Adj-R^2	MAE
2003-2004	0.015	-0.148	0.120	0.780	0.24	1.9
2003-2005	0.022	-0.175	0.120	0.613	0.20	2.0
2003-2006	0.022	-0.149	0.128	0.779	0.21	2.1
2003-2007	0.023	-0.183	0.133	0.760	0.23	2.1
2003-2008	0.021	-0.157	0.157	0.836	0.24	2.1
2003-2009	0.021	-0.201	0.143	0.812	0.25	2.2
2004-2005	0.025	-0.191	0.189	1.161	0.38	2.1
2004-2006	0.017	-0.247	0.153	0.951	0.30	2.2
2004-2007	0.020	-0.184	0.149	0.977	0.27	2.2
2004-2008	0.017	-0.230	0.151	0.950	0.29	2.2
2004-2009	0.020	-0.206	0.159	1.006	0.28	2.2
2005-2006	0.017	-0.173	0.166	0.847	0.28	2.3
2005-2007	0.025	-0.172	0.200	0.921	0.30	2.1
2005-2008	0.018	-0.216	0.168	0.886	0.28	2.2
2005-2009	0.021	-0.175	0.160	0.928	0.26	2.2
2006-2007	0.027	-0.251	0.120	0.844	0.30	2.1
2006-2008	0.023	-0.165	0.166	0.854	0.26	2.2
2006-2009	0.023	-0.221	0.170	0.853	0.29	2.2
2007-2008	0.038	-0.173	0.135	0.351	0.18	2.3
2007-2009	0.026	-0.198	0.123	0.734	0.22	2.3
2008-2009	0.033	-0.157	0.171	0.874	0.28	2.3
Mean	0.023	-0.189	0.152	0.844		
SD	0.005	0.030	0.022	0.155		
RSD	23%	16%	15%	18%		

MLR Residual analysis

An underlying assumption in applying MLR analysis to Eq. (15) is that residuals, defined as the difference between predicted and observed $\Delta\theta$, are normal distributed, time-invariant and there is no serial correlation of residuals (*Kumar and Panu*, 1997). An example of this normality test is shown in Figure 17 using Eq. (15). The normal Q-Q plot (Fig. 17-a) shows that the estimated residual quantiles (y) are linearly correlated with the theoretical quantiles (x), indicating that the residuals are approximately normally distributed. Figure 17-(b) examines if the residuals have any temporal variation. The clear absent of a trend suggests the residuals are independent of time periods of datasets used in the MLR. Figure 17-(c), showing the autocorrelation of the residuals at lag-1, indicates no self-correlation among the residuals.
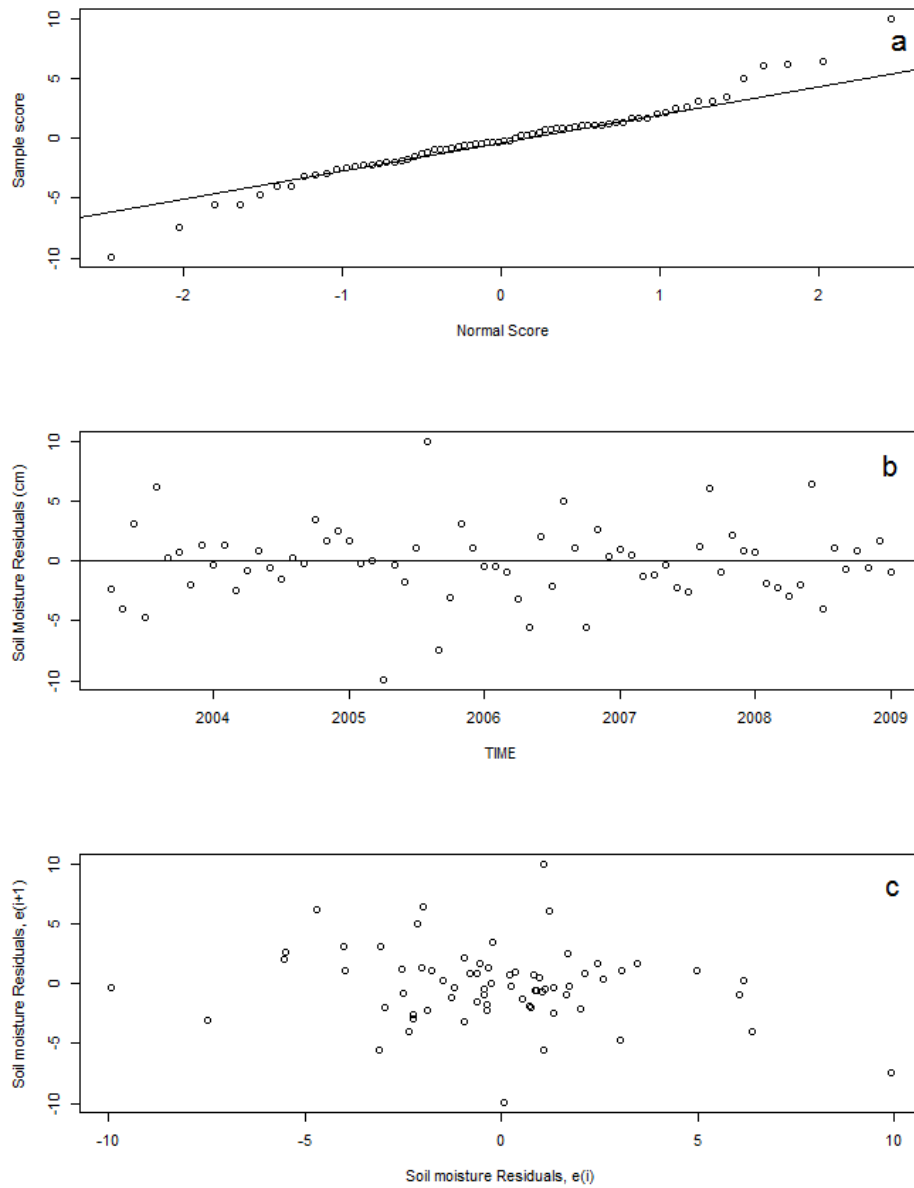
Figure 17 Analysis of the residuals estimated using Eq. (15). (a) Q-Q plot of estimated residual quantiles vs. theoretical normal distribution quantiles. (b) The residuals vs. time periods over which the MLR analysis was performed. (c) Scatter plot between residuals at time t and $t+1$ as serial correlation evaluation.

The coefficients estimated from MLR based on dataset from 2003 to 2009 at one month lead time were applied to predict soil moisture change from 2010 to 2012 for validation. The scatter plot in Figure 18 shows the comparison of predicted soil moisture change and NOAH LSM simulated soil moisture change, which we used to calculate SMDI for drought monitoring. The range of soil moisture change based on MLR is also smaller than the NOAH LSM. A linear fit was applied to evaluate the soil moisture change values estimated by MLR model and the slope is 0.35. The lower than 1 slope suggests that MLR based soil moisture change underestimated its value and it is less sensitive to the extreme conditions. The histogram of the bias between the two data (MLR-NOAH LSM) is normally distributed.
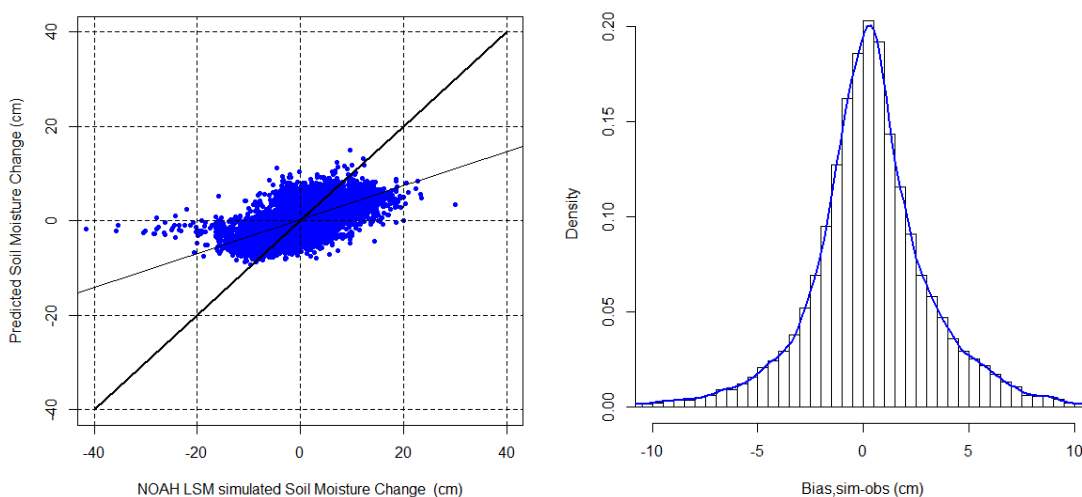
Figure 18 Comparison between soil moisture change estimated by MLR model and NOAH LSM simulation. The bold line in scatter plot is 1:1 line and the solid line is a linear fit of the two with a slope of 0.35. The histogram is the bias between them (MLR-NOAH LSM).

Figure 19 shows the spatial averaged soil moisture change time series between NOAH simulation and the MLR model. Generally, the two datasets share the same temporal pattern. Same as the scatter plot in Figure 18, the MLR based soil moisture

change shows smaller range than the NOAH simulation, with soil moisture change values

ranging from -2 cm to 2 cm. NOAH simulated soil moisture change ranges from -3 cm to

3 cm. generally, the MLR based soil moisture change fits the Noah simulation and it can

be applied to calculate SMDI for drought prediction.
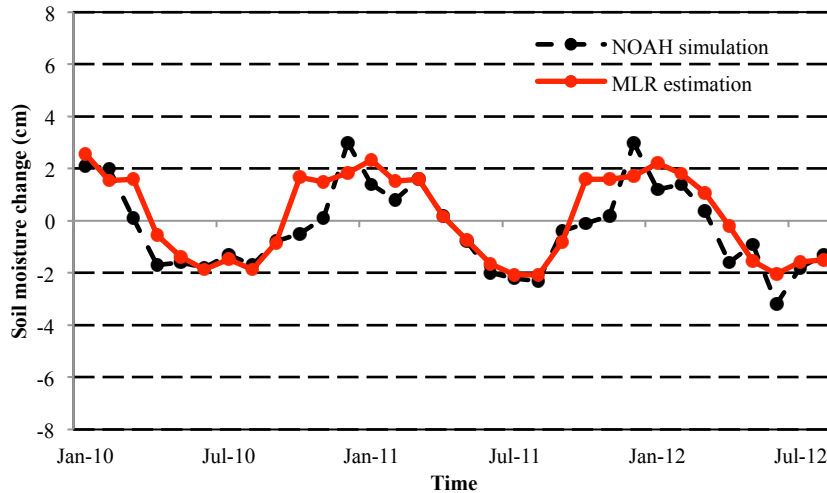
Figure 19 Comparison of spatial averaged soil moisture change from NOAH simulation

and MLR model from 2010 to 2012

From the analysis above, the relation between soil moisture change and other

components retrieved from data between 2003 and 2009 was validated. The estimated

soil moisture change from 2010 to 2012 well captured the temporal pattern during the

severe drought event. It may indicate that the relation between soil moisture change and

P, ET, ΔTWS at one- and two- month lead are stable at different wetness conditions. By

combining the three variables, we are able to estimate soil moisture change at different

conditions. To better understand it, the MLR model was also applied to time spans from

2004 to 2010 and 2005 to 2011, during which, the severest drought of the century

occurred and developed in the southern CONUS. The coefficients are relatively stable

based on the different time spans (Table 6). Soil moisture change estimated based on different time spans also shows no significant differences. Therefore, the coefficients obtained in this study can also used in future estimation and prediction.

Table 6 Coefficients of MLR for different time spans from 2003 to 2009, from 2004 to 2010 and from 2005 to 2011

	P_t	P_{t-1}	ET_t	ET_{t-1}	ΔTWS_t	ΔTWS_{t-1}	season
2003-2009	0.173	-0.149	-0.796	0.598	0.113	0.056	0.525
2004-2010	0.152	-0.15	-0.795	0.678	0.137	0.056	0.557
2005-2011	0.156	-0.154	-0.713	0.62	0.1541	0.06	0.694

SMDI drought prediction

The soil moisture change values were used to calculate the predicted SMDI. The predicted SMDI values were then compared with the monthly SMDI values estimated from the monitoring and the comparison was evaluated using correlation coefficient R and normalized root mean square error (NRMSE). The NRMSE is the RMSE normalized by the range of SMDI (−4 to 4).

Figure 20 shows the performance of the predicted SMDI at one month lead from January 2010 to August 2012 over the CONUS. The plots are close to the one to one line suggesting high accuracy of prediction. The histogram in Figure 23 shows that it agreed well with the monitored SMDI in general (R > 0.9 and NRMSE ~7%±3%). For the current drought period, the predicted SMDI seems performing better in the winter months (October – March) than in the summer months (April – September) (R = 0.98, NRMSE = 5% vs. R = 0.93, NRMSE =9.5%). Yoon et al (2011) developed a Dynamic-Model-Based prediction of SPI based on precipitation forecasts from National Center for Environmental Prediction (NCEP) Climate Forecast system (CFS) over the CONUS.

Interestingly, they also found a seasonally dependent forecast skill in their SPI model, with better performance in winter than in summer. They found an significant contrast in the Great Plain, where the NRMSE in winter season is only 5%, while the NRMSE reaches 15% in summer. They indicated that the reason caused summer forecasting a big error is because of the rainy season.
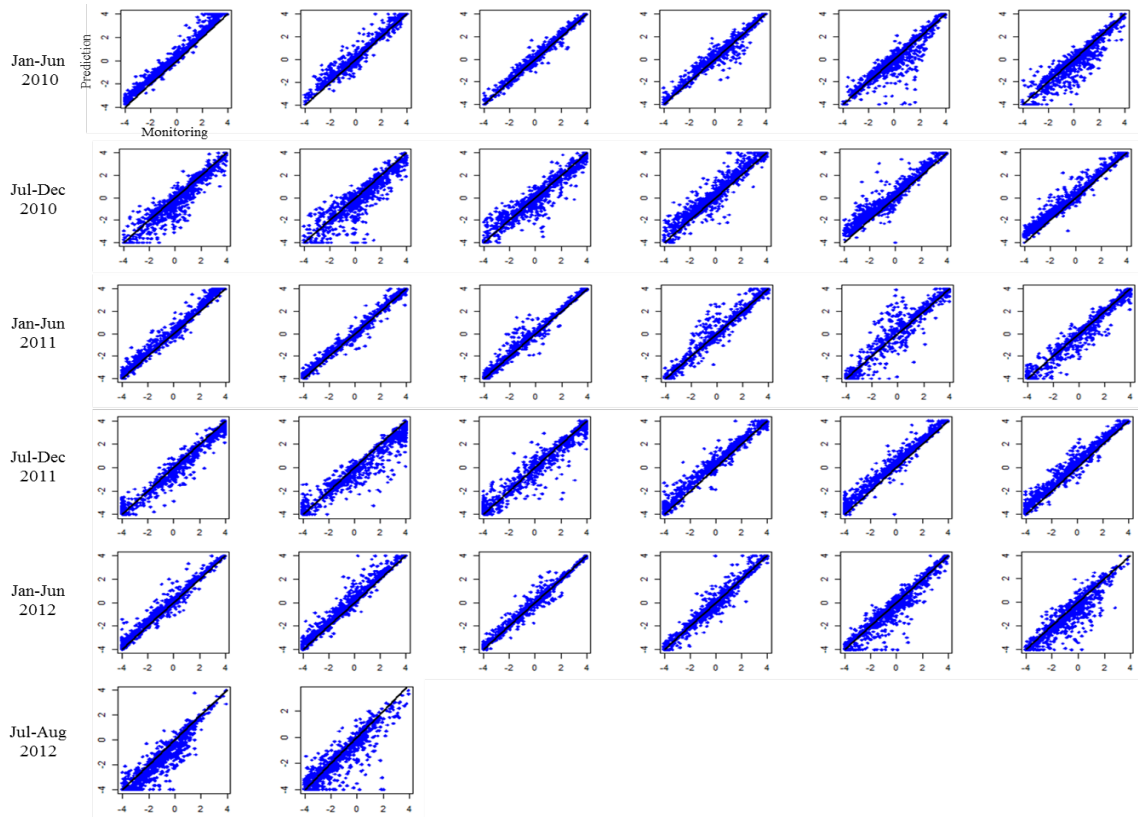
Figure 20 Monthly comparisons from January to August 2012 of SMDI between prediction and observation over the CONUS. Also shown in in each panel are the 1:1 line (black)
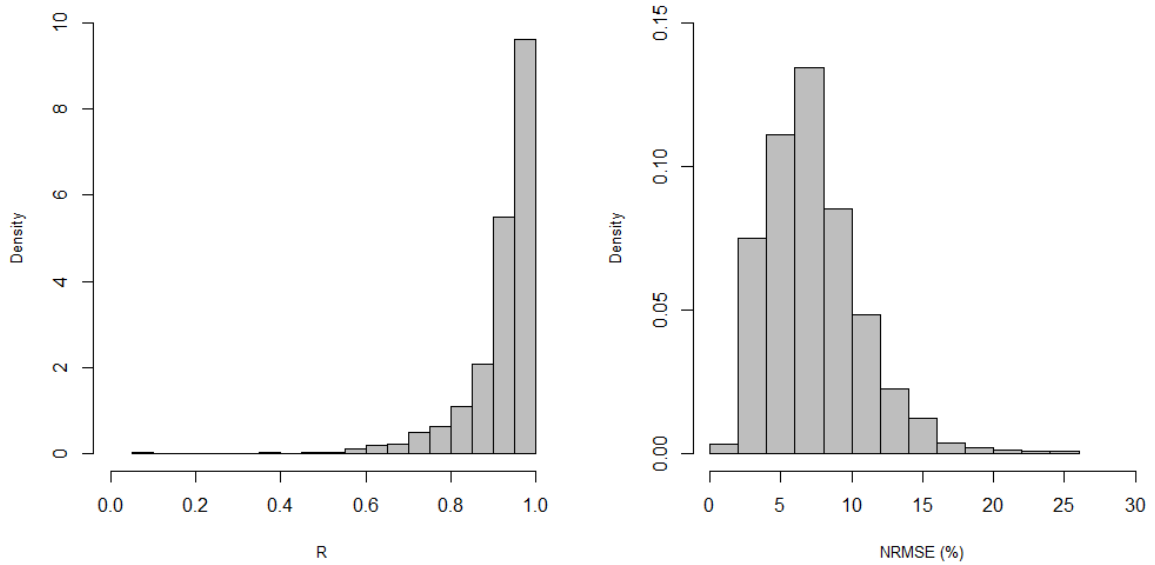
Figure 21 Monthly comparisons from January to August 2012 of SMDI between prediction and observation over the CONUS. Also shown are historgram of the correlation coefficient (R) and the normalized root mean square error (NRMSE) of the comparisons. The NRMSE is estimated as the ratio of RMSE to the range of the SMDI (-4 to 4).

Figure 22 further examines the model performance spatially. Both NRMSE (Fig. 22-a) and R (Fig. 22-b) distributions indicate that the model performed well over the entire CONUS. High correlation coefficient R were observed in the central and western US (R>0.9), However, relatively greater difference was found in the Southeast region as compared with the western and centeral regions. Also, the correlation is low in northwestern and Arizona. NRMSE is low (NRMSE<12%) in most of the CONUS, except southeastern areas. Luo and Wood (2007) compared the agriculatual drought prediction accuraies in eastern and western US and they also reported a lower accuracy in southeastern US. They suggested it is because of the large spread ensemble range in those regions. It may be caused by high variation of the climate conditions in these areas.
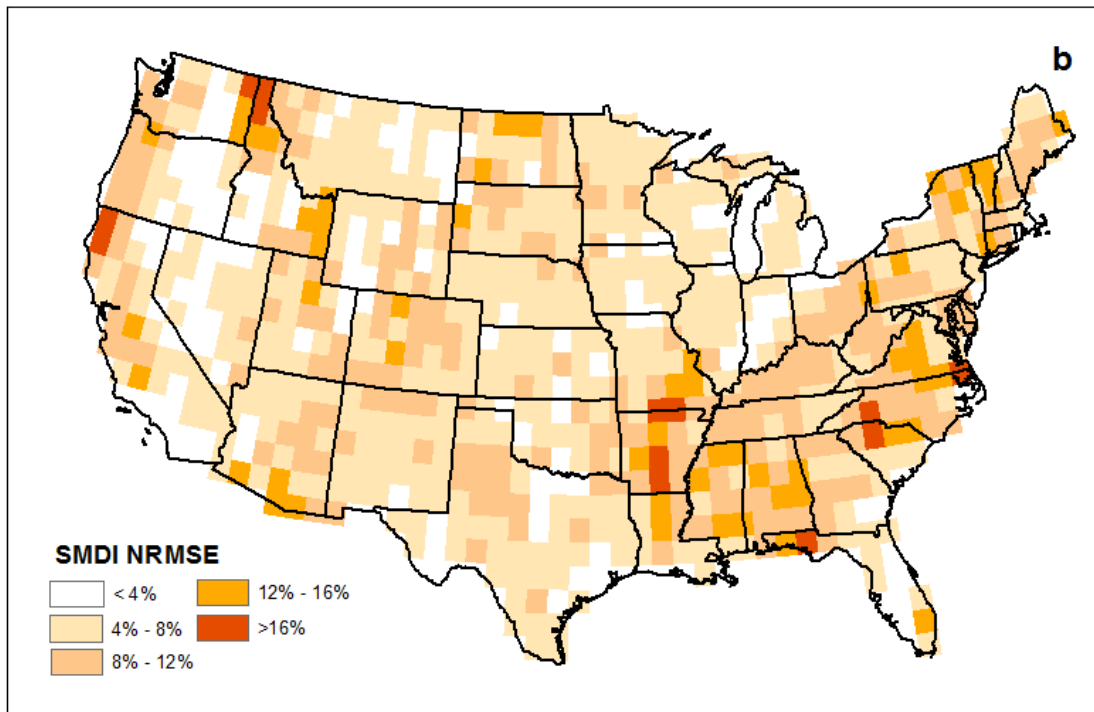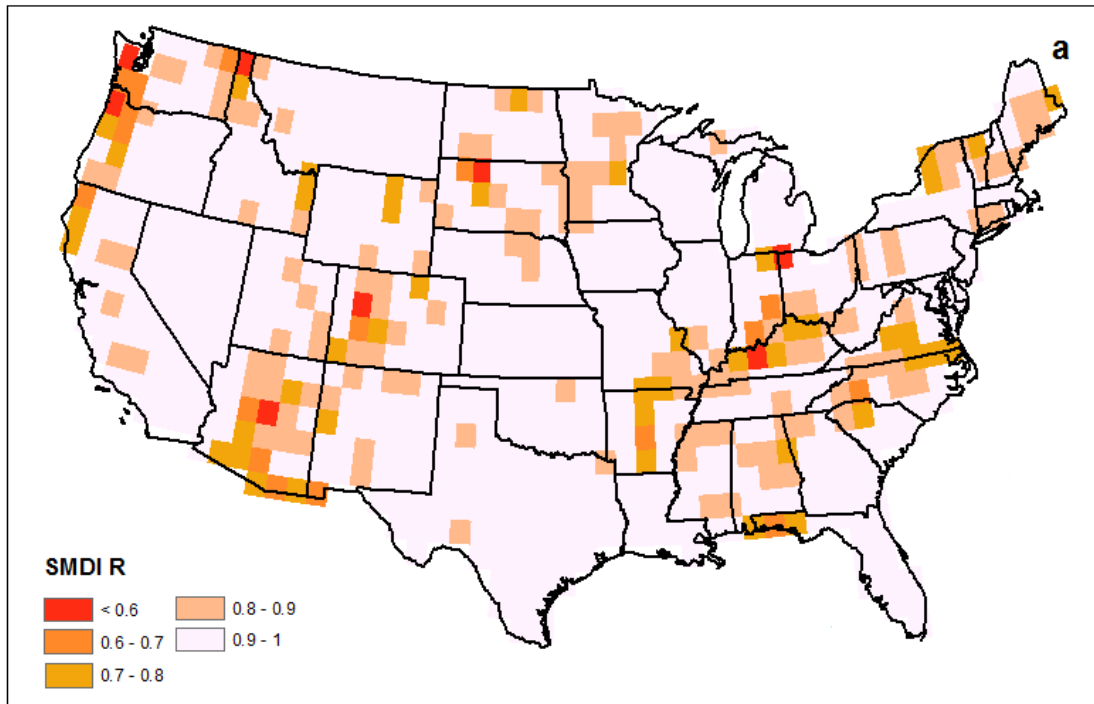
Figure 22. Spatial distribution of correlation coefficient R (a) and NRMSE (b) in evaluating the predictive skill of the developed MLR drought model over the CONUS from 2010 to 2012

Figure 23 compares drought predictions by our MLR model at one- and two-month leads and Luo and Wood (*Luo and Wood*, 2007) (LW07). VIC model at 0.5-, 1.5- and 2.5-month leads with the USDM (*Svoboda et al.*, 2002) for the months of January to August in 2012. The USDM reports three major drought events that took place in Minnesota, Texas-New Mexico and Florida in the first quarter of 2012. After a brief alleviation, the drought continued in June 2012 and expanded to almost the entire CONUS during July and August, resulting one of the most severe droughts in the US. The one-month lead time prediction by our model succesfully captured this major drought event occuring in Minnesota, Texas-New Mexico and Florida in early 2012 and its gradual alliveation during May and June 2012. While the LW07 model successfully captured the drought evolution in general, it failed to forecast the drought in Texas-New Mexico in spring 2012, which is the worst in the history of Texas (*Combs*, 2012). In the summer season, our prediction also compared well with the observed drought index showing the expansion of drought from south to central US. Similar to the one-month lead prediction, the two-month lead prediction also succesfully captured the three major droughts in winter 2012 and their recovery during spring and summer seasons. Compared to the one-month lead prediction, our two-month lead prediction generally underestimates the drought severity, particularly in the eastern US. The 0.5-month lead forecast from LW07 also predicted well the drought expansion in the summer 2012, however, the 1.5- and 2.5- month-lead predictions did not.
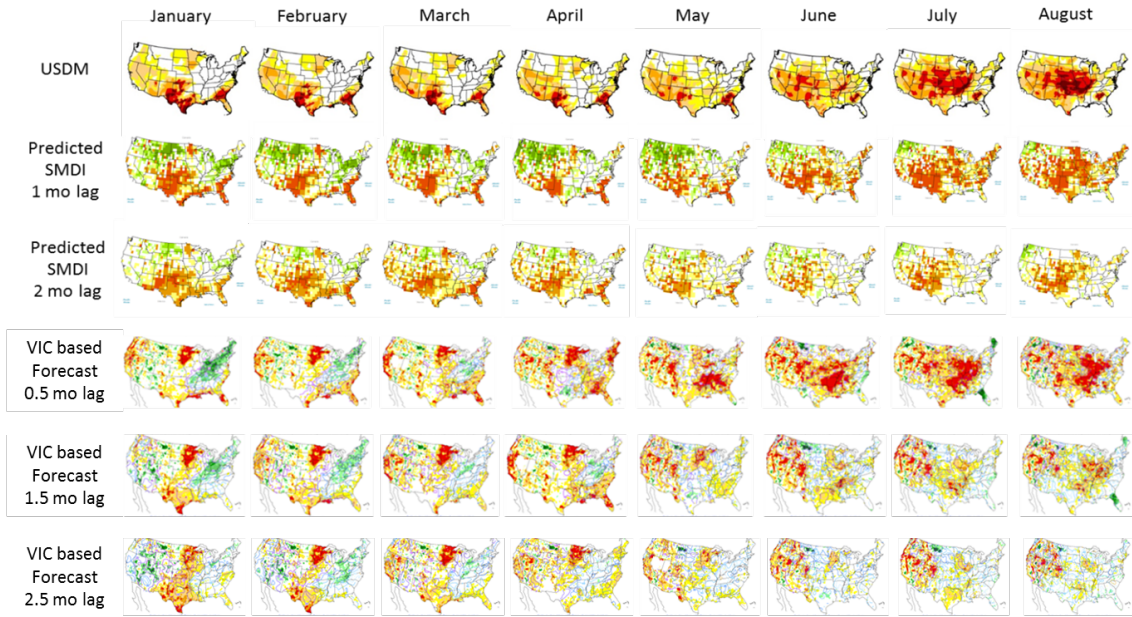
Figure 23 Comparison of drought development monitored by the USDM, predicted at one- and two-month lead by our MLR model (using SMDI as a proxy), and predicted by LW07 model at 0.5-, 1.5- and 2.5-month lead from January to August 2012 over the coninental US. Despite the subtle difference in color scales, the redder the color is, the more severe the drought, and the greener the wetter. Note that the USDM does not provide estimates of wet condition.

Since predicted SMDI performs well in short term drought prediction, we increased initial time to six months.The coefficient to estimage soil moisture change from $t+2$ to $t+6$ are listed below:

Table 7 MLR estimated coefficients for P, ET and ΔTWS for soil moisture change at 2- to 6-month lead times

	P_t	P_{t-1}	ET_t	ET_{t-1}	ΔTWS_t	ΔTWS_{t-1}	Season
lag2	-0.027	0.019	-0.799	0.786	0.065	-0.061	0.110
lag3	-0.021	0.012	-0.534	0.645	-0.043	-0.128	0.106
lag4	-0.027	0.019	-0.154	0.340	-0.107	-0.188	0.058
lag5	-0.031	0.026	0.122	0.075	-0.159	-0.215	-0.034
lag6	-0.005	0.003	0.393	-0.236	-0.190	-0.198	-0.089

The predicted SMDIs are used correlation coefficient and NRMSE to evaluated the accuracy. Figure 24 shows the predictive skill of the model at lead times from one to six months. Relatively speaking, our model had a reasonable forecast skill with up to 2-month leads (R > 0.8 and NRMSE < 15%), whereas with very limited skill beyond a season (R < 0.8 and NRMSE > 20%). The prediction at six-month lag shows low accuracy (R=0.55, NRMSE=29%). This is expected because, as shown in Figure 18, the self-correlation of the hydrological variables we used degraded significantly at a time lag of three months or longer, which can be related to the seasonal pattern of the hydrological variables. Yoon et al (2011) reported their NRMSE between observed and predicted SPI is 12% at one month lead and increases to 27.5% at six month lead. orid et al (2007) compared the prediction skills of Effective Drought Index (EDI) and SPI based on artificial neural networks (ANN), and they found a superior performance when using EDI network model, which has R of 0.9 and NRMSE around 10% with one month lead time. With the lead time increasing to 6 months, the NRMSE increased slightly to 12%. However, this analysis was only applied to Mehrabad station in northern Iran, and they didn't not provide the results for larger areas. Comparing with these drought models, The MLR model that we developed performed better with short-term prediction while the dynamic- model- based forecast and ANN method may have a superior performance with long-term prediciton.
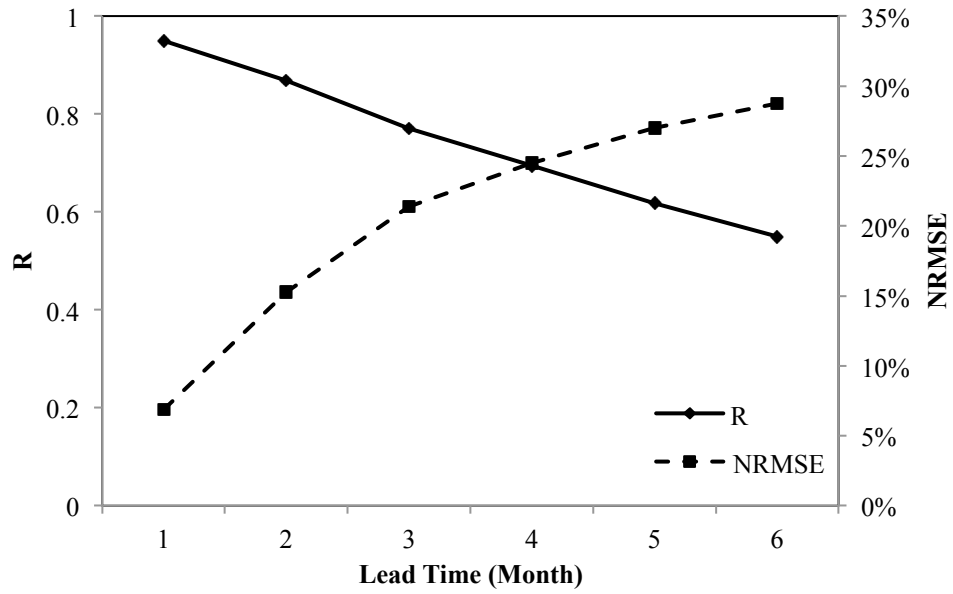
Figure 24. SMDI forecasts evaluation with lag time from one to six month

CHAPTER VI

DISCUSSION

Drought indices used to estimate agricultural drought must have the following characteristics(*Narasimhan and Srinivasan*, 2005): firstly, the indices must be sensitive to the short-term dry conditions, which cause the occurrence of agricultural drought. The SMDI well estimated the dry conditions in southern US during fall and winter 2010, which later developed to an extreme drought in 2011. Secondly, drought indices should be comparable cross seasons. The method of SMD calculation (Eq. 2) removes the seasonality from the soil moisture by extracting the median of soil moisture and normalized by the range of historical data. Therefore the SMDI is able to estimate drought events irrespective of the seasons. Thirdly, drought indices should be spatially comparable. Although drought usually affects large areas, it is still a regional event. The same amount of precipitation, evapotranspiration level or even water content causes different wetness conditions in different regions, due to the variety of land cover, soil texture, terrain, water capacity, and groundwater table. In this study, the SMDI values are spatially comparable because the calculation of the index at each grid cell is independent. The SMDI at one grid cell is only derived from the historical value at this specific grid cell. Therefore SMDI is good for agricultural drought monitoring.

SMDI was first used to evaluate agricultural drought severity in six small watersheds in Texas. The SMDI shows high correlation with PDSI and SPI. However, the

SMDI has never been used to evaluate large scaled areas. The comparison with USDM in this study indicates that SMDI is suited to monitor drought evolutions on large scaled areas. Drought severity discrepancies in the spatial distribution are also observed between the two indices. Since SMDI only monitors agricultural drought and USDM gives the information of meteorological, agricultural, and hydrological, those severity differences are expected. The differences between the two indices could be the result of meteorological and hydrological drought impact. Generally, SMDI performs well in monitoring drought evolutions, particularly in the current severe drought event.

To predict SMDI, an MLR model was applied to predict soil moisture change, which is the key variable for SMDI calculation. Soil moisture deficit, a well defined hydro-physical quantity, represents mass balance of water inputs and outputs, mainly including precipitation, evapotranspiration, runoff, and infiltration. The mass balance not only establishes the underlying physical mechanisms but indicates overall linearities between soil moisture deficit as predictant and precipitation, evapotranspiration, runoff, and infiltration as predictors. Even though our MLR model does not include the terms of runoff and infiltration, the essence of mass balance is largely retained. Specifically, we included the information of seasonality and watersheds into the MLR model, and these two explanatory variables can provide an approximate constraint for the missing terms of runoff and infiltration.

Although the predicted soil moisture change has some limitation on predicting extreme conditions, the predicted SMDIs well capture the drought evolution. The reason behind it could be that SMDI in current month highly relies on the condition in the perious month. In SMDI calculation (Eq 1), q represents the contribution of current soil

moisture deficit conditions to the SMDI. Most of the *q* values are lower than 0.3, which indicates that only one-third of its value depends on the current drought condition. P values, which indicates the contribution of previous SMDI are higher than 0.8. It suggests that drought is a creeping phenomenon. The *p* and *q* values are comparable with PDSI. *Palmer* (1965) also denote a one third weight of current moisture condition and a higher weights of 0.89 from preious PDSI. For two month lead prediction, the SMDI underestimates the drought condition. The reason could be the discrepancy accumulation of the soil moisture change from the model. The predicted SMDI outperforms the predition from LW07 in the 2010 to 2012 drought. The difference could come from different model inputs. In this study, all the climatic and hydrological data are based on observations. LW07 ensembled predicted precipitation and temperature data simulated from different dynamic models and use the ensemble results as the inputs of VIC model. The difference could also come from the models.

SMDI values in growing season show high correlation with crop yields (*Narasimhan and Srinivasan*, 2005). Well predicted SMDI can help predict crop yields before growing seasons and help with decision making and mitigation.

CHAPTER VII

CONCLUSION, LIMITATION AND FUTURE WORK

The CONUS experienced a severe drought from 2010 to 2012. This study shows the usefulness of the SMDI (*Narasimhan and Srinivasan*, 2005) on drought monitoring on large scale in this drought event. The SMDI was compared with USDM products for evaluation. The two datasets shows similar spatial and temporal pattern especially during the most recent severe drought event. Therefore it is reasonable to build a prediction method based on SMDI.

The MLR model shows high stability, and the coefficients (except for ΔTWS at two months lead, which contributes little to soil moisture change) obtained based on different time spans are quite stable with RSD lower than 15%. All these explanatory variables improved the predictive skill of the model, with ET exerting the most significant impact on the model results. ΔTWS derived from GRACE represents total moisture changes in both surface and deep terrestrial layers, with changes in surface layer dominant over short time periods (*Rodell and Famiglietti*, 2001). Inclusion of ΔTWS as an explanatory variable provides an additional physical constraint of the MLR model, even though statistically it only resulted in an improvement in predictive skill of ~7%, probably due to relatively slow *TWS* variation and quick soil moisture response to atmospheric forcing (*Houborg et al.*, 2012).

As the most important indicator of agricultural drought, soil moisture exhibits high spatial and temporal variability. Therefore, it is challenging to predict these parameters. Yet, the MLR model we developed performed well in predicting the change of soil moisture and the drought severity, particularly at short terms of one and two-month lead times. Most remarkably, the model was able to predict a rare yet severe drought event of 2010-2012 and its evolution in the CONUS. Our model was able to predict some detailed development of the 2010-2012 drought event that has eluded a more complex model, LW07, which uses predicted precipitation and temperature to drive a land surface model for soil moisture prediction.

The limitation of this study is the short duration of the GRACE data. In the past century, there were five significant droughts, in 1930s, 1950s, 1980s, 1990s and 2010s. More events can be used for validation if GRACE data is available. The predicted soil moisture change fails to capture the extreme condition in some states, and it may caused by high spatial variability of land surface charactoristics, such as land cover, terrain and soil types at sub grid level.

Further improvement can be expected by examining the model in different regions with different hydrological conditions. In addition, due to the complexity of the hydrological process, data at a finer spatial resolution are also needed to better study drought events. Since agricultural drought during growing season have significant impact on crop yield, a weekly is more suited to estimate and predict moisture conditions during growing season. *Narasimhan and Srinivasan* (2005) found higheast correlation between the SMDI and different crop yields such as sorghum and winter wheat in different weeks during the growing season. Since all the data used in this study has

weekly or even finer temporal resolution, further study can be conducted to look at the relation between agricultual drought prediction and crop yields variation during the growing season.

REFERENCES

Adams, D. K., and A. C. Comrie (1997), The north American monsoon, *Bull. Am. Meteorol. Soc.*, *78*(10), 2197-2213.

Agboma, C. O., S. Z. Yirdaw, and K. R. Snelgrove (2009), Intercomparison of the total storage deficit index (TSDI) over two Canadian Prairie catchments, *J. Hydrol.*, *374*(3–4), 351-359, doi:10.1016/j.jhydrol.2009.06.034.

Alkama, R., B. Decharme, H. Douville, M. Becker, A. Cazenave, J. Sheffield, A. Voldoire, S. Tyteca, and P. Le Moigne (2010), Global Evaluation of the ISBA-TRIP Continental Hydrological System. Part I: Comparison to GRACE Terrestrial Water Storage Estimates and In Situ River Discharges, *J. Hydrometeorol.*, *11*(3), 583-600, doi:10.1175/2010JHM1211.1.

Alley, W. M. (1984), The Palmer Drought Severity Index: limitations and assumptions, *Journal of Climate & Applied Meteorology*, *23*(7), 1100-1109.

Andersen, O. B., and J. Hinderer (2005), Global inter-annual gravity changes from GRACE: Early results, *Geophys. Res. Lett.*, *32*(1), L01402, doi:10.1029/2004gl020948.

Andersen, O. B., S. I. Seneviratne, J. Hinderer, and P. Viterbo (2005), GRACE-derived terrestrial water storage depletion associated with the 2003 European heat wave, *Geophys. Res. Lett.*, *32*(18), L18405, doi:10.1029/2005gl023574.

Angstrom, A. (1925), The Albedo of Various Surfaces of Ground, *Geografiska Annaler*, *7*(ArticleType: research-article / Full publication date: 1925 / Copyright © 1925 Swedish Society for Anthropology and Geography), 323-342, doi:10.2307/519495.

Arulsudar, N., N. Subramanian, and R. Murthy (2005), Comparison of artificial neural network and multiple linear regression in the optimization of formulation parameters of leuprolide acetate loaded liposomes, *J. Pharm. Pharmaceut. Sci*, *8*(2), 243-258.

Baker, J., and R. Allmaras (1990), System for automating and multiplexing soil moisture measurement by time-domain reflectometry, *Soil Sci. Soc. Am. J.*, *54*(1), 1-6.

Baxter, M. A., C. E. Graves, and J. T. Moore (2005), A Climatology of Snow-to-Liquid

Ratio for the Contiguous United States, *Weather and Forecasting*, *20*(5), 729-744, doi:10.1175/WAF856.1.

Becker, M., W. Llovel, A. Cazenave, A. Güntner, and J.-F. Crétaux (2010), Recent hydrological behavior of the East African great lakes region inferred from GRACE, satellite altimetry and rainfall observations, *C.R. Geosci.*, *342*(3), 223-233, doi:http://dx.doi.org/10.1016/j.crte.2009.12.010.

Bosch, D. D., V. Lakshmi, T. J. Jackson, M. Choi, and J. M. Jacobs (2006), Large scale measurements of soil moisture for validation of remotely sensed data: Georgia soil moisture experiment of 2003, *Journal of Hydrology*, *323*(1-4), 120-137.

Bowers, S. A., and S. J. Smith (1972), Spectrophotometric Determination of Soil Water Content1, *Soil Sci. Soc. Am. J.*, *36*(6), 978-980, doi:10.2136/sssaj1972.03615995003600060045x.

Chang, T. J., and X. A. Kleopa (1991), a proposed method for drought monioring, *JAWRA Journal of the American Water Resources Association*, *27*(2), 275-281, doi:10.1111/j.1752-1688.1991.tb03132.x.

Chen, F., K. Mitchell, J. Schaake, Y. Xue, H.-L. Pan, V. Koren, Q. Y. Duan, M. Ek, and A. Betts (1996), Modeling of land surface evaporation by four schemes and comparison with FIFE observations, *J. Geophys. Res.*, *101*(D3), 7251-7268, doi:10.1029/95JD02165.

Chen, F., D. N. Yates, H. Nagai, M. A. LeMone, K. Ikeda, and R. L. Grossman (2003), Land Surface Heterogeneity in the Cooperative Atmosphere Surface Exchange Study (CASES-97). Part I: Comparing Modeled Surface Flux Maps with Surface-Flux Tower and Aircraft Measurements, *J. Hydrometeorol.*, *4*(2), 196-218, doi:10.1175/1525-7541(2003)4<196:lshitc>2.0.co;2.

Chen, X., and Q. Hu (2004), Groundwater influences on soil moisture and surface evaporation, *J. Hydrol.*, *297*(1), 285-300.

Clark, J. S., E. C. Grimm, J. J. Donovan, S. C. Fritz, D. R. Engstrom, and J. E. Almendinger (2002), Drought Cycles and Landscape Responses to past Aridity on Prairies of the Northern Great Plains, USA, *Ecology*, *83*(3), 595-601.

Clausen, B., and C. P. Pearson (1995), Regional frequency analysis of annual maximum streamflow drought, *J. Hydrol.*, *173*(1–4), 111-130, doi:http://dx.doi.org/10.1016/0022-1694(95)02713-Y.

Combs, S. (2012), The Impact of the 2011 Drought and Beyond*Rep. 96-1704*, 16 pp, Texas

Comptroller of Public Accounts, Austin, Texas.

Cordery, I., and M. McCall (2000), A model for forecasting drought from teleconnections, *Water Resour. Res.*, *36*(3), 763-768, doi:10.1029/1999wr900318.

Dai, A. (2011), Drought under global warming: a review, *Wiley Interdisciplinary Reviews: Climate Change*, *2*(1), 45-65, doi:10.1002/wcc.81.

Dai, Y., et al. (2003), The Common Land Model, *Bull. Am. Meteorol. Soc.*, *84*(8), 1013-1023, doi:10.1175/BAMS-84-8-1013.

Dalal, R. C., and R. J. Henry (1986), Simultaneous Determination of Moisture, Organic Carbon, and Total Nitrogen by Near Infrared Reflectance Spectrophotometry1, *Soil Sci. Soc. Am. J.*, *50*(1), 120-123, doi:10.2136/sssaj1986.03615995005000010023x.

Daly, C., M. Halbleib, J. I. Smith, W. P. Gibson, M. K. Doggett, G. H. Taylor, J. Curtis, and P. P. Pasteris (2008), Physiographically sensitive mapping of climatological temperature and precipitation across the conterminous United States, *Int. J. Climatol.*, *28*(15), 2031-2064.

Economic Research Service (2013), Irrigation & Water Use, edited.

Ek, M. B., K. E. Mitchell, Y. Lin, E. Rogers, P. Grunmann, V. Koren, G. Gayno, and J. D. Tarpley (2003), Implementation of Noah land surface model advances in the National Centers for Environmental Prediction operational mesoscale Eta model, *J. Geophys. Res. [Atmos.]*, *108*(D22), 8851, doi:10.1029/2002jd003296.

ERS (2002), Major Uses of Land in the United States, 2002, edited.

Famiglietti, J. S., M. Lo, S. L. Ho, J. Bethune, K. J. Anderson, T. H. Syed, S. C. Swenson, C. R. de Linage, and M. Rodell (2011), Satellites measure recent rates of groundwater depletion in California's Central Valley, *Geophys. Res. Lett.*, *38*(3), L03403, doi:10.1029/2010GL046442.

Fan, Y., H. M. Van den Dool, D. Lohmann, and K. Mitchell (2006), 1948–98 U.S. Hydrological Reanalysis by the Noah Land Data Assimilation System, *J. Clim.*, *19*(7), 1214-1237, doi:10.1175/jcli3681.1.

Fannin, B. (2012), Texas Agricultural Drought Losses Reach Record $5.2 Billion*Rep.*, Texas Agrilife Extension Service.

Federal Emergency Management Agency (1995), National Mitigation Strategy: Partnerships for Biolding Safer Communities*Rep.*, 44 pp, Government Printing Office, Washington, DC.

Figa-Saldaña, J., J. J. Wilson, E. Attema, R. Gelsthorpe, M. Drinkwater, and A. Stoffelen (2002),

The advanced scatterometer (ASCAT) on the meteorological operational (MetOp) platform: A follow on for European wind scatterometers, *Can. J. Remote Sens.*, *28*(3), 404-412.

Freedman, A. (2012), Causes Of Midwest Drought: La Nina And Global Warming Thought To Contribute To Dry Weather in *Huffington Post.* , edited.

Gibbs, W. J., and J. V. Maher (1967), Rainfall deciles as drought indicators *Bureau of Meteorology*.

Güntner, A. (2008), Improvement of Global Hydrological Models Using GRACE Data, *Surv. Geophys.*, *29*(4-5), 375-397, doi:10.1007/s10712-008-9038-y.

Guttman, N. B. (1999), ACCEPTING THE STANDARDIZED PRECIPITATION INDEX: A CALCULATION ALGORITHM1, *JAWRA Journal of the American Water Resources Association*, *35*(2), 311-322, doi:10.1111/j.1752-1688.1999.tb03592.x.

Hartmann, H. C., T. C. Pagano, S. Sorooshian, and R. Bales (2002), Confidence Builders: Evaluating Seasonal Climate Forecasts from User Perspectives, *Bull. Am. Meteorol. Soc.*, *83*(5), 683.

Hayes, M. J., D. Svoboda, D. A. Wilhite, and O. V. Vanyarkho (1999), Monitoring the 1996 drought using the standardized precipitation index, *Bull. Am. Meteorol. Soc.*, *80*(3), 429-438.

Heim , R., Jr. (2002), A review of twentieth-century drought indices used in the United States, *Bull. Am. Meteorol. Soc.*, *83*, 1149-1165.

Hinderer, J., O. Andersen, F. Lemoine, D. Crossley, and J.-P. Boy (2006), Seasonal changes in the European gravity field from GRACE: A comparison with superconducting gravimeters and hydrology model predictions, *J. Geodyn.*, *41*(1–3), 59-68, doi:http://dx.doi.org/10.1016/j.jog.2005.08.037.

Houborg, R., M. Rodell, B. Li, R. Reichle, and B. F. Zaitchik (2012), Drought indicators based on model-assimilated Gravity Recovery and Climate Experiment (GRACE) terrestrial water storage observations, *Water Resour. Res.*, *48*(7), W07525, doi:10.1029/2011WR011291.

Hu, Q., S. Feng, H. Guo, G. Chen, and T. Jiang (2007), Interactions of the Yangtze river flow and hydrologic processes of the Poyang Lake, China, *J. Hydrol.*, *347*(1–2), 90-100, doi:http://dx.doi.org/10.1016/j.jhydrol.2007.09.005.

Karamouz, M., K. Rasouli, and S. Nazif (2009), Development of a Hybrid Index for Drought Prediction: Case Study, *Journal of Hydrologic Engineering*, *14*(6), 617-627, doi:doi:10.1061/(ASCE)HE.1943-5584.0000022.

Keyantash, J., and J. A. Dracup (2002), The Quantification of Drought: An Evaluation of Drought Indices, *Bull. Am. Meteorol. Soc.*, *83*(8), 1167-1180, doi:10.1175/1520-0477(2002)083<1191:tqodae>2.3.co;2.

King, M. D., and R. Greenstone (1999), 1999 EOS reference handbook: a guide to NASA's Earth Science Enterprise and the Earth Observing System, *1999 EOS reference handbook: a guide to NASA's Earth Science Enterprise and the Earth Observing System, by King, Michael D.; Greenstone, Reynold. Greenbelt, Md.: NASA/Goddard Space Flight Center,[1999]*, *1*.

Koster, R. D., and M. J. Suarez (1992), Modeling the land surface boundary in climate models as a composite of independent vegetation stands, *J. Geophys. Res.*, *97*(D3), 2697-2715, doi:10.1029/91jd01696.

Kumar, V., and U. Panu (1997), Predictive assessment of severity of agricultural droughts based on agro-climatic factors *JAWRA Journal of the American Water Resources Association*, *33*(6), 1255-1264, doi:10.1111/j.1752-1688.1997.tb03550.x.

Landerer, F. W., and S. C. Swenson (2012), Accuracy of scaled GRACE terrestrial water storage estimates, *Water Resour. Res.*, *48*(4), W04531, doi:10.1029/2011WR011453.

Ledieu, J., P. De Ridder, P. De Clerck, and S. Dautrebande (1986), A method of measuring soil moisture by time-domain reflectometry, *J. Hydrol.*, *88*(3), 319-328.

Li, B., M. Rodell, B. F. Zaitchik, R. H. Reichle, R. D. Koster, and T. M. van Dam (2012), Assimilation of GRACE terrestrial water storage into a land surface model: Evaluation and potential value for drought monitoring in western and central Europe, *J. Hydrol.*, *446*, 103-115.

Liang, X., D. P. Lettenmaier, E. F. Wood, and S. J. Burges (1994a), A simple hydrologically based model of land surface water and energy fluxes for general circulation models, *J. Geophys. Res.*, *99*(D7), 14415-14428, doi:10.1029/94jd00483.

Liang, X., D. P. Lettenmaier, E. F. Wood, and S. J. Burges (1994b), A simple hydrologically based model of land surface water and energy fluxes for general circulation models, *J. Geophys. Res.*, *99*(D7), 14415-14428.

Liu, W. T., and R. I. N. Juárez (2001), ENSO drought onset prediction in northeast Brazil using NDVI, *Int. J. Remote Sens.*, *22*(17), 3483-3501, doi:10.1080/01431160010006430.

Luo, L., and E. F. Wood (2007), Monitoring and predicting the 2007 U.S. drought, *Geophys. Res. Lett.*, *34*(22), L22702, doi:10.1029/2007gl031673.

Mahrt, L., and H. Pan (1984), A two-layer model of soil hydrology, *Boundary-Layer Meteorology*, *29*(1), 1-20.

Manabe, S. (1969), Climate and the ocean circulation: 1. The atmospheric circulation and the hydrology of the earth's surface, *Monthly Weather Review*, *97*, 739-805.

Marsh, T. (2007), The 2004–2006 drought in southern Britain, *Weather*, *62*(7), 191-196, doi:10.1002/wea.99.

McCumber, M. C., and R. A. Pielke (1981), Simulation of the effects of surface fluxes of heat and moisture in a mesoscale numerical model: 1. Soil layer, *Journal of Geophysical Research: Oceans*, *86*(C10), 9929-9938, doi:10.1029/JC086iC10p09929.

McKee, T. B., N. J. Doesken, and J. Kleist (1993a), The relationship of drought frequency and duration to time scales, paper presented at Proceedings of the 8th Conference on Applied Climatology, American Meteorological Society Boston, MA.

McKee, T. B., N. J. Doesken, and J. Kliest (1993b), The relationship of drought frequency and duration to time scales., in *Proceedings of the 8th Conference of Applied Climatology*, edited, pp. 179-184, Meterological Society, Boston, MA, Anaheim, CA.

Mishra, A. K., and V. P. Singh (2010), A review of drought concepts, *J. Hydrol.*, *391*(1–2), 202-216, doi:http://dx.doi.org/10.1016/j.jhydrol.2010.07.012.

Modarres, R., and A. Sarhadi (2010), Frequency Distribution of Extreme Hydrologic Drought of Southeastern Semiarid Region, Iran, *Journal of Hydrologic Engineering*, *15*(4), 255-264, doi:doi:10.1061/(ASCE)HE.1943-5584.0000186.

Moran, M. S., C. D. Peters-Lidard, J. M. Watts, and S. McElroy (2004), Estimating soil moisture at the watershed scale with satellite-based radar and land surface models, *Can. J. Remote Sens.*, *30*(5), 805-826, doi:10.5589/m04-043.

Morid, S., V. Smakhtin, and K. Bagherzadeh (2007), Drought forecasting using artificial neural networks and time series of drought indices, *Int. J. Climatol.*, *27*(15), 2103-2111, doi:10.1002/joc.1498.

Mu, Q., F. A. Heinsch, M. Zhao, and S. W. Running (2007), Development of a global

evapotranspiration algorithm based on MODIS and global meteorology data, *Remote Sens. Environ.*, *111*(4), 519-536.

Mu, Q., M. Zhao, and S. W. Running (2011), Improvements to a MODIS global terrestrial evapotranspiration algorithm, *Remote Sens. Environ.*, *115*(8), 1781-1800, doi:http://dx.doi.org/10.1016/j.rse.2011.02.019.

Narasimhan, B., and R. Srinivasan (2005), Development and evaluation of Soil Moisture Deficit Index (SMDI) and Evapotranspiration Deficit Index (ETDI) for agricultural drought monitoring, *Agr. Forest Meteorol.*, *133*(1–4), 69-88, doi:10.1016/j.agrformet.2005.07.012.

NCDC (2006), Each state's low temperature record, edited.

NDMC (2006), What is drought? Understanding and Defining Drought, edited, National Climatic Data Center.

Niu, G.-Y., and Z.-L. Yang (2006), Assessing a land surface model's improvements with GRACE estimates, *Geophys. Res. Lett.*, *33*(7), L07401, doi:10.1029/2005gl025555.

Niu, G.-Y., Z.-L. Yang, R. E. Dickinson, L. E. Gulden, and H. Su (2007), Development of a simple groundwater model for use in climate models and evaluation with Gravity Recovery and Climate Experiment data, *J. Geophys. Res.*, *112*(D7), D07103, doi:10.1029/2006jd007522.

Noilhan, J., and S. Planton (1989), A Simple Parameterization of Land Surface Processes for Meteorological Models, *Monthly Weather Review*, *117*(3), 536-549, doi:10.1175/1520-0493(1989)117<0536:aspols>2.0.co;2.

Ntale, H. K., and T. Y. Gan (2003), Drought indices and their application to East Africa, *Int. J. Climatol.*, *23*(11), 1335-1357, doi:10.1002/joc.931.

Pacific Disaster Center (2013), Understanding and Defining Drought, edited.

Palmer, W. C. (1965), *Meteorological Drought*, Office of Climatology U.S. Weather Bureau, Washington, D.C.

Palmer, W. C. (1968), Keeping track of crop moisture conditions, nationwide: The new crop moisture index, *Weatherwise*, *21*, 156-161.

Pan, H. L., and L. Mahrt (1987), Interaction between soil hydrology and boundary-layer development, *Boundary-Layer Meteorology*, *38*(1-2), 185-202, doi:10.1007/bf00121563.

Paulo, A., and L. Pereira (2007), Prediction of SPI Drought Class Transitions Using Markov

Chains, *Water Resour. Manage.*, *21*(10), 1813-1827, doi:10.1007/s11269-006-9129-9.

Proulx, R. A., M. D. Knudson, A. Kirilenko, J. A. VanLooy, and X. Zhang (2013), Significance of surface water in the terrestrial water budget: A case study in the Prairie Coteau using GRACE, GLDAS, Landsat, and groundwater well data, *Water Resour. Res.*, *49*(9), 5756-5764, doi:10.1002/wrcr.20455.

Qiu, Y., B. Fu, J. Wang, and L. Chen (2003), Spatiotemporal prediction of soil moisture content using multiple-linear regression in a small catchment of the Loess Plateau, China, *Catena*, *54*(1–2), 173-195, doi:http://dx.doi.org/10.1016/S0341-8162(03)00064-X.

Quiring, S. M., and T. N. Papakryiakou (2003), An evaluation of agricultural drought indices for the Canadian prairies, *Agr. Forest Meteorol.*, *118*(1–2), 49-62, doi:10.1016/s0168-1923(03)00072-8.

Ramillien, G., F. Frappart, A. Güntner, T. Ngo-Duc, A. Cazenave, and K. Laval (2006), Time variations of the regional evapotranspiration rate from Gravity Recovery and Climate Experiment (GRACE) satellite gravimetry, *Water Resour. Res.*, *42*(10), W10403, doi:10.1029/2005wr004331.

Rangelova, E., W. van der Wal, A. Braun, M. G. Sideris, and P. Wu (2007), Analysis of Gravity Recovery and Climate Experiment time-variable mass redistribution signals over North America by means of principal component analysis, *Journal of Geophysical Research: Earth Surface*, *112*(F3), F03002, doi:10.1029/2006jf000615.

Rhee, J., J. Im, and G. J. Carbone (2010), Monitoring agricultural drought for arid and humid regions using multi-sensor remote sensing data, *Remote Sens. Environ.*, *114*(12), 2875-2887, doi:http://dx.doi.org/10.1016/j.rse.2010.07.005.

Rijal, S., X. Zhang, and X. Jia (2013), Estimating Surface Soil Water Content in the Red River Valley of the North using Landsat 5 TM Data, *Soil Sci. Soc. Am. J.*

Rodell, M., J. Chen, H. Kato, J. Famiglietti, J. Nigro, and C. Wilson (2007), Estimating groundwater storage changes in the Mississippi River basin (USA) using GRACE, *Hydrogeology Journal*, *15*(1), 159-166, doi:10.1007/s10040-006-0103-7.

Rodell, M., and J. S. Famiglietti (2001), An analysis of terrestrial water storage variations in Illinois with implications for the Gravity Recovery and Climate Experiment (GRACE), *Water Resour. Res.*, *37*(5), 1327-1339, doi:10.1029/2000wr900306.

Rodell, M., and J. S. Famiglietti (2002), The potential for satellite-based monitoring of

groundwater storage changes using GRACE: the High Plains aquifer, Central US, *J. Hydrol.*, *263*(1–4), 245-256, doi:http://dx.doi.org/10.1016/S0022-1694(02)00060-4.

Rodell, M., J. S. Famiglietti, J. Chen, S. I. Seneviratne, P. Viterbo, S. Holl, and C. R. Wilson (2004a), Basin scale estimates of evapotranspiration using GRACE and other observations, *Geophys. Res. Lett.*, *31*(20), L20504, doi:10.1029/2004gl020873.

Rodell, M., et al. (2004b), The Global Land Data Assimilation System, *Bull. Am. Meteorol. Soc.*, *85*(3), 381-394, doi:10.1175/bams-85-3-381.

Roth, C. H., M. A. Malicki, and R. Plagge (1992), Empirical evaluation of the relationship between soil dielectric constant and volumetric water content as the basis for calibrating soil moisture measurements by TDR, *J. Soil Sci.*, *43*(1), 1-13, doi:10.1111/j.1365-2389.1992.tb00115.x.

Sadeghi, A. M., G. D. Hancock, W. P. Waite, H. D. Scott, and J. A. Rand (1984), Microwave Measurements of Moisture Distributions in the Upper Soil Profile, *Water Resour. Res.*, *20*(7), 927-934, doi:10.1029/WR020i007p00927.

Santos, M. A. (1983), Regional droughts: A stochastic characterization, *J. Hydrol.*, *66*(1–4), 183-211, doi:http://dx.doi.org/10.1016/0022-1694(83)90185-3.

Scanlon, B. R., L. Longuevergne, and D. Long (2012), Ground referencing GRACE satellite estimates of groundwater storage changes in the California Central Valley, USA, *Water Resour. Res.*, *48*(4), W04520, doi:10.1029/2011wr011312.

Schaake, J. C., V. I. Koren, Q.-Y. Duan, K. Mitchell, and F. Chen (1996), Simple water balance model for estimating runoff at different spatial and temporal scales, *J. Geophys. Res.*, *101*(D3), 7461-7475, doi:10.1029/95jd02892.

Schmidt, R., F. Flechtner, U. Meyer, K. H. Neumayer, C. Dahle, R. König, and J. Kusche (2008), Hydrological Signals Observed by the GRACE Satellites, *Surv. Geophys.*, *29*(4-5), 319-334, doi:10.1007/s10712-008-9033-3.

Sheffield, J., G. Goteti, F. Wen, and E. F. Wood (2004), A simulated soil moisture based drought analysis for the United States, *J. Geophys. Res.*, *109*(D24), D24108, doi:10.1029/2004jd005182.

Sirdas, S., and Z. Sen (2003), Spatio-temporal drought analysis in the Trakya region, Turkey, *Hydrol. Sci. J.*, *48*(5), 809-820, doi:10.1623/hysj.48.5.809.51458.

Sivakumar, M., and D. Wilhite (2002), Drought preparedness and drought management, paper

presented at International Conference on Drought Mitigation and Prevention of Land Desertification.

Sridhar, V., R. L. Elliott, F. Chen, and J. A. Brotzge (2002), Validation of the NOAH-OSU land surface model using surface flux measurements in Oklahoma, *J. Geophys. Res.*, *107*(D20), 4418, doi:10.1029/2001jd001306.

Svoboda, M., et al. (2002), The Drought Monitor, *Bull. Am. Meteorol. Soc.*, *83*(8), 1181-1190.

Swenson, S., J. Wahr, and P. C. D. Milly (2003), Estimated accuracies of regional water storage variations inferred from the Gravity Recovery and Climate Experiment (GRACE), *Water Resour. Res.*, *39*(8), 1223, doi:10.1029/2002wr001808.

Syed, T. H., J. S. Famiglietti, J. Chen, M. Rodell, S. I. Seneviratne, P. Viterbo, and C. R. Wilson (2005), Total basin discharge for the Amazon and Mississippi River basins from GRACE and a land-atmosphere water balance, *Geophys. Res. Lett.*, *32*(24), L24404, doi:10.1029/2005gl024851.

Syed, T. H., J. S. Famiglietti, M. Rodell, J. Chen, and C. R. Wilson (2008), Analysis of terrestrial water storage changes from GRACE and GLDAS, *Water Resour. Res.*, *44*(2), W02433.

Tapley, B. D., S. Bettadpur, J. C. Ries, P. F. Thompson, and M. M. Watkins (2004a), GRACE Measurements of Mass Variability in the Earth System, *Science*, *305*(5683), 503-505, doi:10.1126/science.1099192.

Tapley, B. D., S. Bettadpur, M. Watkins, and C. Reigber (2004b), The gravity recovery and climate experiment: Mission overview and early results, *Geophys. Res. Lett.*, *31*(9), L09607, doi:10.1029/2004gl019920.

Tiwari, V. M., J. Wahr, and S. Swenson (2009), Dwindling groundwater resources in northern India, from satellite gravity observations, *Geophys. Res. Lett.*, *36*(18), L18401, doi:10.1029/2009gl039401.

USGS (2013), Science in your watershed, edited.

Van Rooy, M. (1965), A rainfall anomaly index independent of time and space, *Notos*, *14*, 43-48.

Vogt, J. V., and F. Somma (2000), Drought and Drought Mitigation in Europe, paper presented at Hydrogeol. J.

Wahr, J., M. Molenaar, and F. Bryan (1998), Time variability of the Earth's gravity field: Hydrological and oceanic effects and their possible detection using GRACE, *J. Geophys. Res.*, *103*(B12), 30205-30229, doi:10.1029/98jb02844.

Walker, J. P. (1999), Estimating soil moisture profile dynamics from near-surface soil moisture measurements and standard meteorological data, The University of Newcastle.

Walker, J. P., G. R. Willgoose, and J. D. Kalma (2004), In situ measurement of soil moisture: a comparison of techniques, *J. Hydrol.*, *293*(1), 85-99.

Walsh, B. (2011), Drought Cripples the South: Why the 'Creeping Disaster' Could Get a Whole Lot Worse *Time*.

Wells, N. W., S. Goddard, and M. J. Hayes (2004), A self-calibrating Palmer drought severity index, *J. Clim.*, *17*, 2335-2351, doi:citeulike-article-id:3025524.

Werth, S., and A. Güntner (2010), Calibration analysis for water storage variability of the global hydrological model WGHM, *Hydrol. Earth Syst. Sci.*, *14*(1), 59-78, doi:10.5194/hess-14-59-2010.

Wilhite, D. A., and M. H. Glantz (1985), Understanding: the drought phenomenon: the role of definitions, *Water International*, *10*(3), 111-120.

Willmott, C. J. (1981), ON THE VALIDATION OF MODELS, *Physical Geography*, *2*(2), 184-194, doi:10.1080/02723646.1981.10642213.

Winsemius, H. C., H. H. G. Savenije, A. M. J. Gerrits, E. A. Zapreeva, and R. Klees (2006), Comparison of two model approaches in the Zambezi river basin with regard to model reliability and identifiability, *Hydrol. Earth Syst. Sci.*, *10*(3), 339-352, doi:10.5194/hess-10-339-2006.

Yeh, P. J. F., S. C. Swenson, J. S. Famiglietti, and M. Rodell (2006), Remote sensing of groundwater storage changes in Illinois using the Gravity Recovery and Climate Experiment (GRACE), *Water Resour. Res.*, *42*(12), W12203, doi:10.1029/2006wr005374.

Yirdaw, S. Z., K. R. Snelgrove, and C. O. Agboma (2008), GRACE satellite observations of terrestrial moisture changes for drought characterization in the Canadian Prairie, *J. Hydrol.*, *356*(1–2), 84-92, doi:10.1016/j.jhydrol.2008.04.004.

Yoon, J.-H., K. Mo, and E. F. Wood (2011), Dynamic-Model-Based Seasonal Prediction of Meteorological Drought over the Contiguous United States, *J. Hydrometeorol.*, *13*(2), 463-482, doi:10.1175/jhm-d-11-038.1.